General Disclaimer

One or more of the Following Statements may affect this Document

- This document has been reproduced from the best copy furnished by the organizational source. It is being released in the interest of making available as much information as possible.

- This document may contain data, which exceeds the sheet parameters. It was furnished in this condition by the organizational source and is the best copy available.

- This document may contain tone-on-tone or color graphs, charts and/or pictures, which have been reproduced in black and white.

- This document is paginated as submitted by the original source.

- Portions of this document are not fully legible due to the historical nature of some of the material. However, it is the best reproduction available from the original submission.

NASA Contractor Report 165469

Development of Low Modulus Material for Use in Ceramic Gas Path Seal Systems

H.E. Eaton
R.C. Novak

United Technologies Research Center
East Hartford, CT 06108

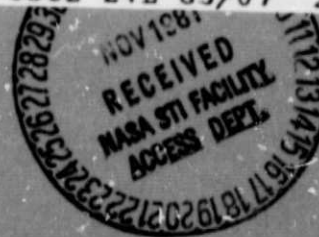## NASA

National Aeronautics and
Space Administration

Lewis Research Center
Cleveland, Ohio 44135

UNITED TECHNOLOGIES RESEARCH CENTER

East Hartford, Connecticut 06108

UNITED TECHNOLOGIES™

NASA CR-165469

Development of Low Modulus Material For
Use in Ceramic Gas Path Seal Systems

H. E. Eaton
R. C. Novak

Final Report

Contract NAS3-22134

October 1981

Development of Low Modulus Material For Use in Ceramic Gas Path Seal Systems

TABLE OF CONTENTS

LIST OF TABLES

LIST OF FIGURES

I. INTRODUCTION

Current turbine outer gas path seal systems based on metallic designs have two prime disadvantages related to performance: excessive cooling requirements and large turbine blade tip clearance. It is necessary to bleed air from the rear section of the compressor of the engine for cooling of metal turbine blade tip seals to maintain them within safe operating temperature limits. This cooling results in an engine performance penalty due to loss of high pressure air from the cycle. The injection of this air into the hot gas flow path also reduces turbine efficiency. Inadvertent rubbing between blade tips and the static seal shroud occurs due to seal shroud distortions, thermal and dynamic transients, and rotor bending when operating with tight clearances. Since present turbine seals for the most part are not abradable, a conservative approach is taken in establishing turbine operating clearnaces to prevent rotor wear. This promotes leakage of high energy air over the blade tips without work being extracted by the blades, thus lowering the turbine efficiency.

Because of these disadvantages associated with metallic systems, ceramic outer gas path seals are under development currently by both industry and government for use in high performance commercial and military aircraft engines. The ceramic seal concept offers two important features which make the system very attractive. First, higher engine operating temperatures are achievable because of the high temperature capability of ceramics coupled with their low thermal conductivity. Second, the ceramic seals can be made to be abradable which leads to improved gas path sealing.

To realize the advantages of ceramic seals, a design must be developed that solves the problem arising from the difference in thermal expansion coefficients between the cobalt or nickel based substrates presently in use and the ceramic layer. This difference can be sufficient to lead to bonding failure in the region of the ceramic-substrate interface.

Presently, two approaches can provide a solution and both are under development. One approach (Ref. 1) involves plasma spraying sequentially graded composition intermediate layers between the substrate and ceramic along with controlling the stress state of the layers. Stress control is necessary since plasma sprayed ceramic/metal systems can fail in a brittle fashion and preloading is seen as a means to increase the durability of the seal system. The other (Ref. 2) involves a low modulus strain isolator cushion between the substrate and ceramic wherein differences in thermal expansion are accommodated by deformation of the low modulus layer.

The objective of this program was to develop and characterize low modulus material systems capable of successfully performing in a seal application at a material temperature of at least 1255°K. The approach involved the evaluation and optimization of three concepts. These are: Brunsbond(R) Pad, plasma sprayed porous metal, and plasma sprayed low modulus ceramic.

The program was divided into four technical tasks. The candidate systems were chosen in Task I. Task II involved the screening of variations of each system. Task III involved detailed property measurements. Task IV involved further investigation of a selected system.

II. TASK I - SELECTION OF CANDIDATE MATERIAL SYSTEMS

2.1 Criteria for Candidate Low Modulus Strain Isolator Systems

The low modulus, strain-isolator interlayer between the metal substrate and ceramic surface layer is the key building block of the ceramic outer gas path seal system.

As a whole the seal system must be designed to withstand the demands of the operating environment. For the interlayer, these demands require that the structural integrity be sufficient for exposure to operational conditions. The interlayer must be capable of withstanding thousands of stress cycles induced by thermal gradients due to engine start-up, shut-down and operation. This is one of the most critical and most difficult requirements to meet. The design of the bonding between the high temperature ceramic surface layer and the metal substrate structure is critical to the success of the seal system. The interlayer must successfully absorb differential thermal expansion and maintain the strains in the ceramic surface layer within allowable limits for all foreseeable thermal cycles. Finally, the interlayer must satisfactorily withstand imposed forces due to vibration, pressure differentials, blade tip rub, hard landings, etc.

The physical properties to define and characterize the strain isolator interlayer include: (1) density, (2) chemistry, and (3) microstructure. These properties provide the basis for control of the system and the basis for the establishment of relationships between the other physical, mechanical, and thermal properties.

The thermal properties which are necessary to determine the temperature and strain distribution throughout the seal system are: (1) thermal conductivity, (2) specific heat, (3) density, and (4) thermal expansion. These properties are critical because the primary source of stress in the low modulus system results from differences in the thermal expansion and differences in temperatures of the ceramic and the metal substrate.

The mechanical properties which are required to determine stress levels within the low modulus system are: (1) modulus of elasticity, (2) strength, and (3) strain capacity. The modulus of elasticity is required to translate the calculated thermal strains into thermal stresses. The strength and strain capabilities of the material are used to define safe limits of operation.

As a result, the NASA selection criteria for this program included the following:

. Potential to attain modulus of elasticity in the range of 3.5 to 6.9 GPa (.5 to 1 MSI), and ultimate strength of 17.2 MPa (2.5 KSI)

. High thermal conductivity

- Static oxidation life of at least 1000 hours at 1311°K.

- Feasibility of attaching the low modulus system to a broad range of substrate alloys

- Feasibility of depositing or forming the low modulus system to thicknesses of 0.2 cm to 0.4 cm (.075" to .150")

Three candidate systems were chosen for evaluation. First the fiber metal Brunsbond[R] Pad concept served as the baseline for the program. The second candidate involved plasma spraying a porous metal layer directly onto a prepared metal substrate. This offered the possibility of more simple fabrication, lower costs, and greater ease of refurbishment than the first approach. The third candidate involved a low modulus ceramic layer plasma sprayed directly onto a prepared substrate.

These approaches, the rationale for proposing them, and the evaluation techniques are discussed more fully in the following four sections.

2.2 Fiber Metal Concept

The low modulus strain isolator approach requires a material that has a lower elastic modulus than the ceramic top layer and metal substrate to allow the ceramic and metal to strain independently of each other to minimize stresses within the structure. A low modulus fiber metal material is commercially available from Brunswick Corporation and possesses the candidate elastic and strength properties (Ref. 3).

Brunswick produces a fiber metal product consisting of 0.142 mm diameter Hoskins 875 fibers in pad form, marketed as Brunsbond[R] Pad. This is available in different densities and thicknesses. Attachment of the pad to a substrate is accomplished by a metallurgical braze process such as with a Nicrobraze foil. A ceramic top layer can then be plasma sprayed directly onto the bondcoated fiber pad surface. Brunsbond[R] Pad is being evaluated by Pratt and Whitney Aircraft-Government Products Division (Ref. 4), by NASA (Ref. 2), and by Brunswick (Ref. 3) for ceramic gas path seal use.

Brunsbond[R] Pad at 35% true density and 2.54 mm thickness was chosen for evaluation as the baseline system in this program. Specimens of 30% and 40% density and 2.54 mm thickness were also considered for possible lower modulus or increased thermal conductivity.

2.3 Plasma Sprayed Porous Metal

The ability of the fiber metal approach to produce a low modulus material is in part due to the attenuation of stiffness as a result of the incorporation of porosity into the metal structure. Another approach to produce a low modulus cushion

4

between the ceramic seal and the metal substrate is to plasma spray a porous metal layer. This approach is very attractive for two reasons. First, plasma spraying technology provides the means to fabricate coatings in a cost and labor efficient manner. Second, plasma spraying technology is under active development as a method to fabricate ceramic seal systems, and consequently, a plasma sprayed low modulus cushion could be integrated readily into a continuous spray process.

Certain requirements must be addressed in considering the fabrication of a plasma sprayed, low modulus, porous metal cushion. These include attachment of the cushion to a wide variety of substrate alloys and the achievement of specified oxidation resistance, and strength, modulus, and coating thickness values. Methods of addressing these requirements within the plasma sprayed porous metal approach are described briefly below.

2.3.1 Attachment Requirements

To attach the plasma sprayed porous coating to substrates of low carbon steel, stainless steel, titanium, and aluminum, a 5 mil thick bond coat should be used, such as a blend of 94 Nichrome/6 aluminum (Metco 443). Metco literature (Ref. 5) values indicate that bond strengths to these substrates are of the order of 4000 psi. Research Center experience indicates that this bond coat material is also applicable to nickel and cobalt based superalloys.

2.3.2 Oxidation Resistance Requirements

Alloys that form an alumina scale on exposure to air at elevated temperatures usually exhibit excellent oxidation properties. The compounds such as NiAl, Ni_3Al, and the materials that are grouped together as MCrAlY, where M is either iron, nickel, or cobalt, fall into this category. In general, the chromium content of MCrAlY varies from about 12 to 25 w/o and the aluminum level is within the range of 4 to 13 w/o. Yttrium at a level of approximately 0.5 w/o is added to enhance scale adherence.

Experience at the Research Center and at NASA (Ref. 6) indicated that the NiCrAlY would be a suitable alloy. The composition chosen for this program was Ni-25Cr-6Al-.36Y.

2.3.3 Property Requirements

Strength and modulus values of porous metal can be affected by controlling the porosity through the incorporation of a fugitive constituent such as polyester. To control the strength and modulus of the porous NiCrAlY, three levels of polyester (Metco 600) were blended with NiCrAlY and sprayed under Task II.

5

2.4 Plasma Sprayed Low Modulus Ceramic

The fiber metal and porous metal approaches to fabricate a low modulus cushion involve metal systems. The third approach involves the use of a plasma sprayed low modulus ceramic layer. A low modulus ceramic layer offers a distinct advantage over the preceding two systems in the area of high temperature oxidation resistance.

Figure 2-1 shows a typical 4 pt bend stress versus strain curve for a plasma sprayed ceramic material of low modulus in which the loading of the system is kept below the fracture strength level. As indicated, the system exhibits both elastic and inelastic behavior as non-recoverable deformation. This behavior is observed also with compression testing. Inelastic behavior at room temperature is atypical of ceramic materials and is the result of the plasma spray process. Sprayed ceramics exhibit markedly different strength and modulus values in addition to distinct microstructures depending on the plasma spray parameters used in fabrication. Low strength-low modulus specimens exhibit both porosity and splat morphology. The loose, mechanically interlocked microstructure is responsible in part for the observed nonlinear behavior in the stress-strain curve. Also, cracks that occur under stressing can be deflected and effectively arrested by the splat morphology. Because of this nonlinear behavior of the plasma sprayed ceramic materials, this approach offered promise, although not without risk, of successfully producing a low modulus plasma sprayed ceramic cushion for this application.

There are at least three possible techniques to influence the strength, modulus, and compliance of a plasma sprayed ceramic. These include adjustment of the plasma spray parameters to affect the microstructure; direct incorporation of porosity through the use of a fugitive such as polyester; and the development of microcracks in the ceramic as the result of the fabrication process. All three techniques were evaluated in Task II with yttria stabilized zirconia (Metco 202 NS) as the ceramic.

2.5 Evaluation Procedures

Evaluation testing was performed on each candidate to guage its ability to perform in a strain isolator configuration. In Task II, data was obtained on the strength and oxidation properties of each. In Tasks III and IV, strength, static and cyclic oxidation behavior, and thermal properties were measured. The microstructure was examined and attachment to a substrate was demonstrated. Machining and testing procedures are described below.

2.5.1 Machining

Special machining techniques are necessary when dealing with porous metals or ceramics because these materials are very susceptible to chipping or cracking during the machining operation. In order to avoid these problems, samples are impregnated with either beeswax or stickwax prior to machining. After the specimens are machined to the desired shapes and dimensions, the wax is removed by dissolution

6

in either tricholoroethylene or methanol, depending upon the type of wax which is used. To insure the removal of small traces of wax that may remain, the specimens are refluxed in the appropriate solvent. For surface finishing, a 320 grit grinding wheel is used.

2.5.2 Tensile Properties

Both room temperature and 1089°K mechanical property tests were performed on samples in both the as-fabricated condition and after static exposure to 1311°K in air for 500 hours. The modulus of elasticity, ultimate tensile strength, and strain to failure were determined for each specimen.

In instances where gripping difficulties were encountered, the specimens underwent 4-point bend tests rather than true tensile tests. For the room temperature tests the strain was determined using a strain gage, and for the elevated temperature tests the strain was determined by use of an extensometer.

2.5.3 Oxidation Testing

Static oxidation testing was carried out at 1311°K in a still air resistance furnace for a duration of 500 hours. Weight gain and dimensional change measurements were made after 1, 10, 100, 200 and 500 hours.

Cyclic oxidation tests were carried out in a specially-made rig which allows for sample movement in and out of a resistance heated tube furnace. The specimens were held at a maximum temperature of 1311°K for 65 minutes and then raised out of the furnace and air cooled for 15 minutes. The total accumulated time at 1311°K was one-hundred (100) hours. Weight gain and dimensional change measurements were made after accumulated times of 1, 10, 50 and 100 hours at 1311°K.

2.5.4 Thermal Conductivity

The thermal conductivity of each material was determined by the Thermophysical Properties Research Laboratory of Purdue University. Each material was tested from room temperature to 1089°K in the thickness direction. The density, specific heat, and thermal diffusivity were measured and the thermal conductivity calculated from these results.

The bulk densities were determined from the mass and geometries of the samples. The specific heat values were measured with a differential scanning calorimeter. Thermal diffusivity values were determined using the laser flash technique.

As described in TPRL Report # 249, the laser flash apparatus consists of a Korad K2 laser, a high vacuum system including a bell jar with windows for viewing the sample, a tantalum tube heater surrounding a sample holding assembly, an IR detector, appropriate biasing circuits, amplifiers, A-D converters, crystal clocks,

and a minicomputer-based digital data acquisition system capable of accurately taking data in the 40 microsecond and longer time domain. In the apparatus a small disc shaped sample of the candidate material is subjected to a short laser burst and the resulting rear face temperature rise is recorded. The computer controls the experiment, collects the data, calculates the results, and compares the new data with the theoretical model.

2.5.5 Microstructural Investigation

The as-fabricated specimens were subjected to metallographic examination in order to determine important microstructural features. The specimens which underwent static oxidation tests and cyclic oxidation tests were also examined.

2.5.6 Attachment Demonstration

Each of the candidate systems was attached to stainless steel and cobalt based alloys to demonstrate attachment feasibility. For the fiber pad, a brazing process was employed, while for the sprayed systems Metco 443 bondcoat was used.

FIG. 2-1

TYPICAL STRESS VS. STRAIN CURVE FOR A PLASMA
SPRAYED CERAMIC OF LOW STRENGTH

(MAXIMUM LOAD ≤ FRACTURE STRENGTH)
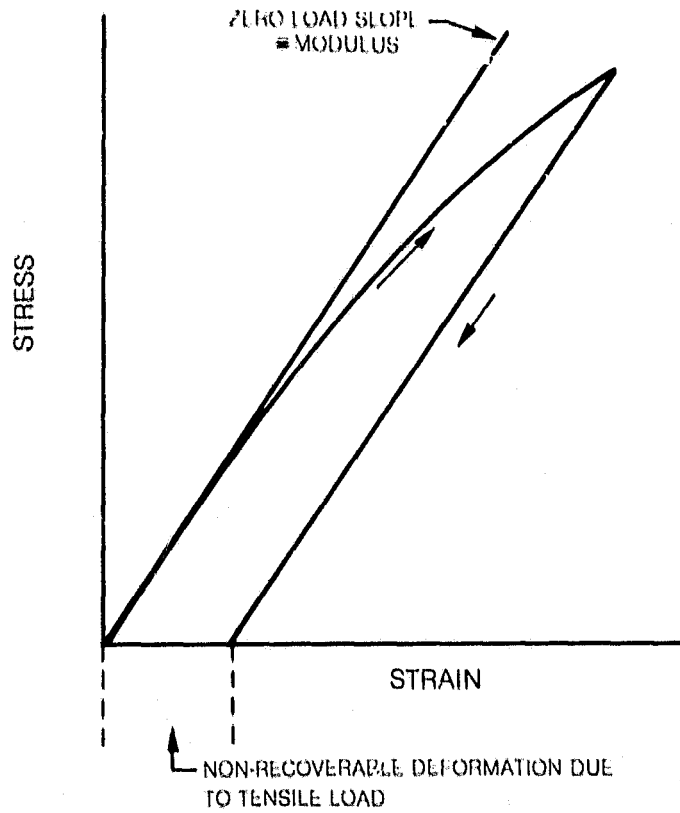
III. TASK II - PRELIMINARY EVALUATION OF SELECTED SYTEMS

Figure 3-1 summarizes the systems along with variations in these systems selected for preliminary evaluation in Task II. The preliminary evaluation conducted in Task II consisted of room temperature mechanical property tests, and static oxidation at 1311°K for 24 hours.

3.1 Fiber Metal Approach

Specimens of Brunsbond[R] Pad were purchased from Brunswick Corp., Deland, FL. The Brunsbond[R] Pads were composed of 0.142 mm fibers of Hoskins 875 alloy sintered together to form different densities. Nominal densities of 30%, 35% and 40% were evaluated.

Mechanical property specimen dimensions were 12.7 cm x 2.54 cm x 0.254 cm. Fiberglass doublers, 4.0 cm in length, were epoxied to the ends of each specimen. The gage length between doublers was 4.7 cm, and attached to the specimen in this region was a 2.54 cm extensometer for strain measurement. Figure 3-2 summarizes the average mechanical properties versus density for the Brunsbond[R] Pads. The actual data are presented in Table A-1.

For these tensile tests, failure generally occurred outside the gage length of the extensometer, and, as a result, strain to failure was reported in most cases as being greater than 1%. In subsequent tensile tests, each doubler component was tapered to promote failure within the gage length.

Static oxidation of the three densities for 24 hours at 1311°K produced less than 0.6% weight gain as indicated in Table A-2.

3.2 Porous NiCrAlY

Specimens of porous NiCrAlY at three different densities (4780, 2870 and 2390 Kg/M^3) were fabricated by plasma spraying blends of polyester and NiCrAlY. The polyester was Metco 600 and the NiCrAlY was Ni-25Cr-6Al-.35Y initially sieved to -170 + 325 mesh, received from Homogeneous Metals, Inc., Clayville, New York. The spray parameters and powder blends are described in Table A-3.

Four point bend mechanical property test specimens of each density were machined out of sprayed monoliths having dimensions of approximately 5 cm x 10 cm x .37 cm. Test specimens were 2.75 cm x 1.0 cm x .25 cm. Prior to mechanical property or oxidation testing, the polyester was baked cut by exposure to 810°K for 1 hour.

Figure 3-3 summarizes the mechanical properties versus density for the porous NiCrAlY. The data are presented in Table A-4. Strain was measured by both a

deflectometer and a strain gage. The difference between strain gage and deflectometer modulus values can be attributed either to machine compliance at low loading for the deflectometer values or to infiltration of the porous NiCrAlY by the strain gage epoxy. The true modulus value probably lies between the two reported values.

Static oxidation is summarized in Fig. 3-4 and the data are presented in Table A-5. Oxidation measurements based on percent weight gain reflect the high surface area of a plasma sprayed porous metal system.

3.3 Low Modulus Ceramic

Specimens of low modulus zirconia were produced having three distinct microstructures. A porous microstructure, Fig. 3-5, was produced by plasma spraying a blend of Metco 600 polyester and Metco 202 NS zirconia. A microcracked microstructure was produced by plasma spraying Metco 202 NS under conditions that produced a controlled amount of microcracking (Fig. 3-6). Work at the Research Center has shown that microcracks can be produced in plasma sprayed zirconia through the control of certain spray parameters such as voltage, amperage, injector configuration and substrate cooling. It is believed that the specimen is thermally shocked continuously during spraying resulting in the microcrack network. In the third technique, a loosely bound microstructure, Fig. 3-7, was produced by plasma spraying Metco 202 NS zirconia with spray parameters selected to accomplish this. In each case monoliths were sprayed having dimensions of approximately 5 cm x 10 cm x .37 cm. From these monoliths, individual 4 point bend specimens were cut having dimensions of 2.75 cm x 1 cm x .25 cm.

Figure 3-8 summarizes the 4-point bend strength and modulus values of these systems. The data are presented in Table A-6.

Static oxidation at 1311°K for 24 hours shows no weight gain. The data are presented in Table A-7.

3.4 Selection of Task III Systems

Based on testing performed under Task II and in conjunction with discussions between the Research Center and the NASA Program Manager, the following three systems were selected for evaluation in Task III.

. Brunsbond[R] Pad at 35% density

. Porous NiCrAlY at 2870 kg/M^3 density

. Microcracked zirconia

Brunsbond[R] Pad at 35% density represented a baseline strain isolator system (Ref. 4). Increased density leads to increased modulus while decreased density is not optimum from a strength viewpoint.

Porous NiCrAlY at 2870 kg/M^3 density represented the best choice based on strength and modulus data. In an attempt to reduce oxidation, a coarser grade of NiCrAlY powder was evaluated early on in Task III.

Microcracked zirconia represented an interesting system since the cracks could be controlled and were oriented in a fashion which might accommodate the differences in thermal expansion between the seal substrate and top layer.

FIG. 3-1

CANDIDATE LOW MODULUS STRAIN ISOLATOR SYSTEMS AND VARIATIONS SELECTED IN TASK I

```
                    ┌─────────────────────┐
                    │      SELECTION      │ ─ ─ ─ ─ ─ ─ TASK I
                    └─────────────────────┘
                              │
          ┌───────────────────┼───────────────────┐
  ┌───────────────┐   ┌───────────────┐   ┌───────────────┐
  │  FIBER PAD    │   │ POROUS NiCrAlY│   │   ZIRCONIA    │
  │ THREE DENSITIES│  │ THREE DENSITIES│  │THREE VARIATIONS│
  └───────────────┘   └───────────────┘   └───────────────┘

   30%  35%  40%       30%  40%  60%      POROUS   LOW    MICRO-
                                                 MODULUS  CRACKED
```

```
                    ┌─────────────────────────┐
                    │       FABRICATION        │
                    │  MECHANICAL PROPERTIES   │ ─ ─ ─ ─ ─ TASK II
                    │  24 OXIDATION AT 1900°F  │
                    └─────────────────────────┘
```

FIG. 3-2
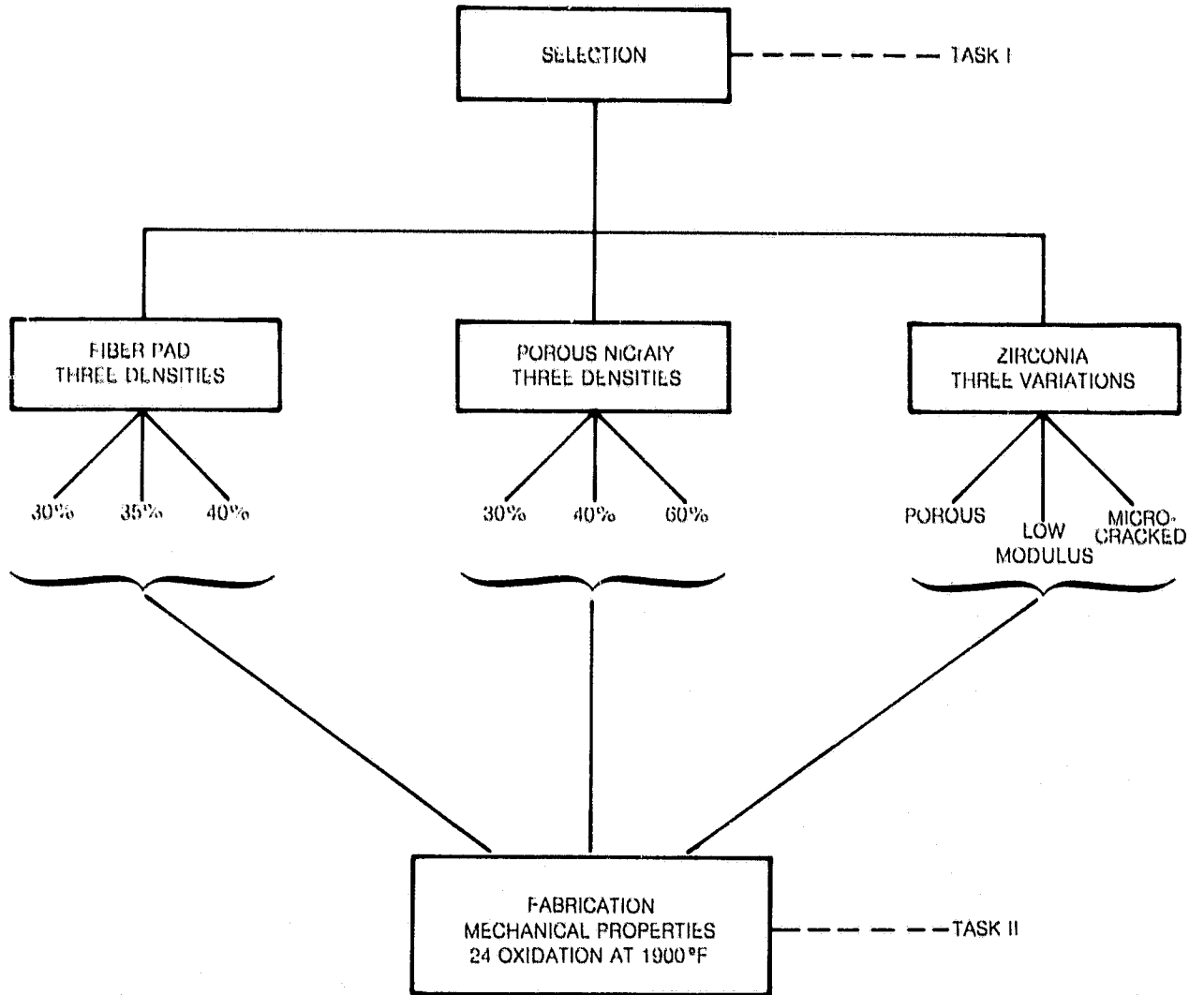
ROOM TEMPERATURE TENSILE PROPERTIES VS DENSITY OF BRUNSBOND⁽ᴬ⁾ PAD

STRENGTH

MODULUS

81—8—92—21

FIG. 3-3
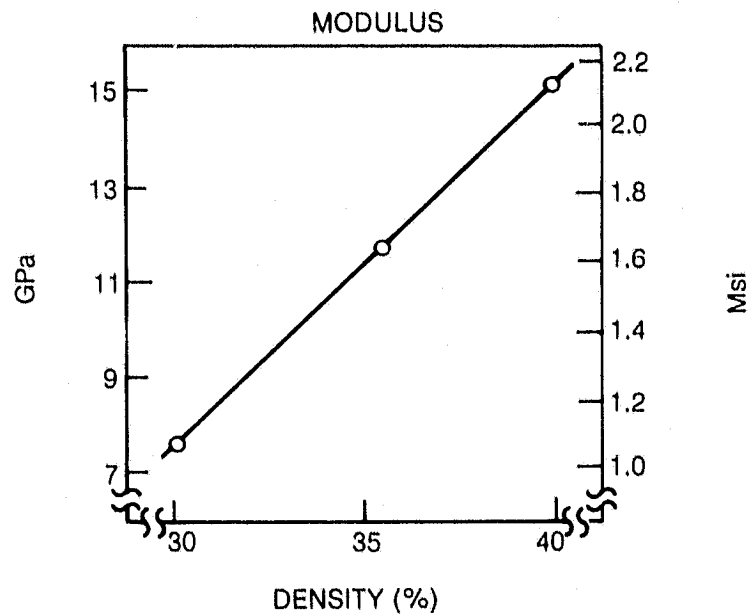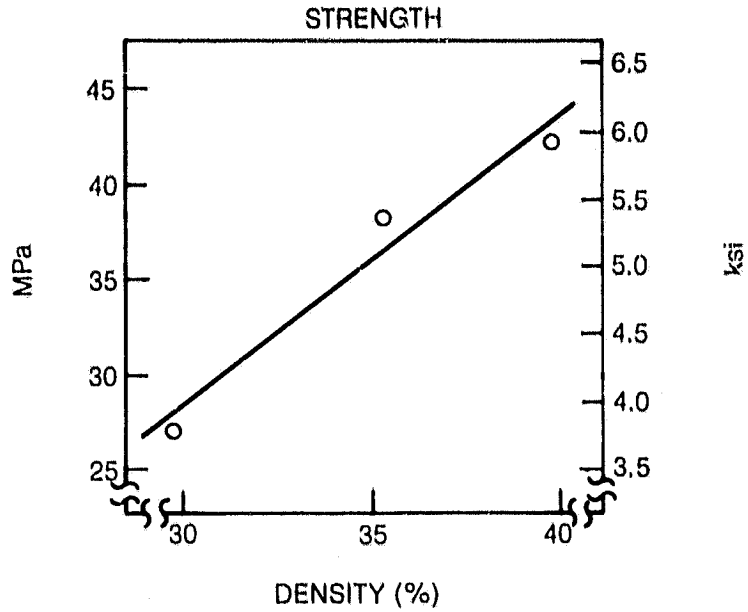
ROOM TEMPERATURE FOUR POINT BEND PROPERTIES OF POROUS NiCrAlY vs DENSITY

STRENGTH

DENSITY (Kg/M^3)

MODULUS

DENSITY (Kg/M^3)

81-8-92-3

15

FIG. 3-4
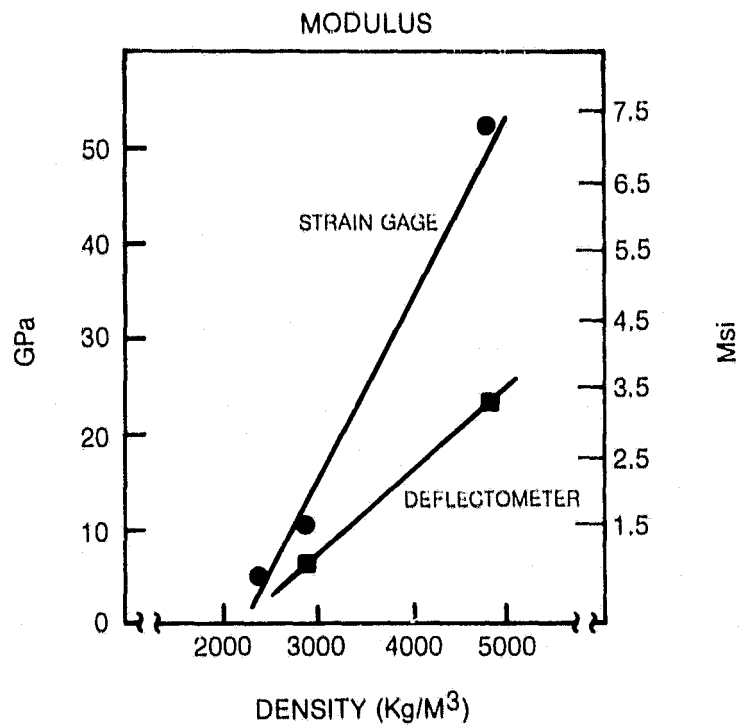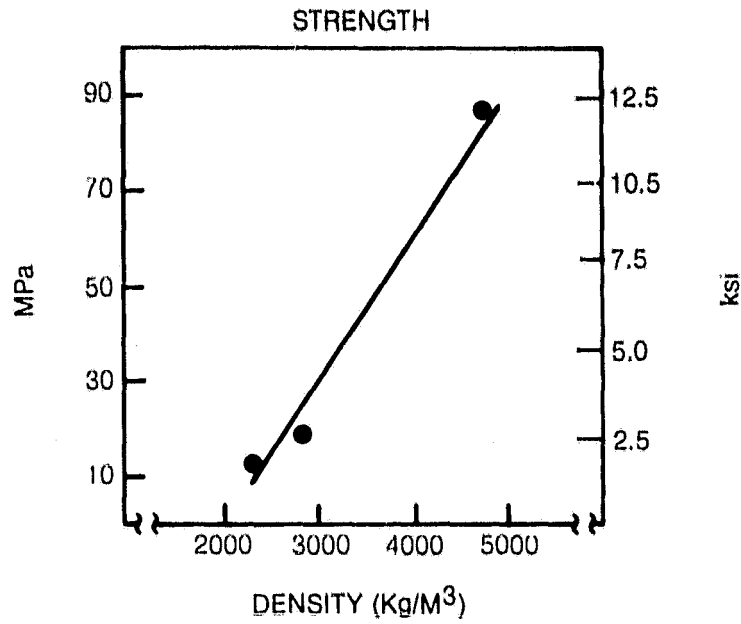
WEIGHT PERCENT OXIDATION POROUS NICrAlY vs DENSITY
AT 1310°K FOR 24 HOURS
(-170 + 325 MESH NICrAlY)

FIG. 3-5
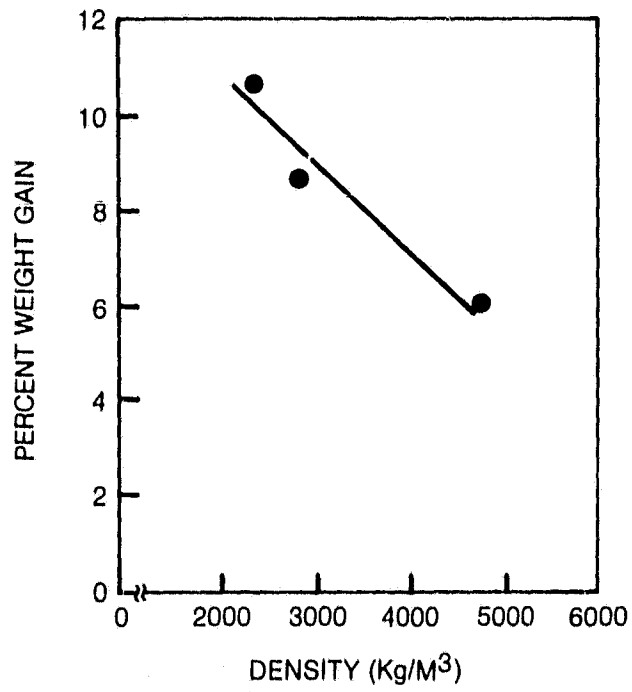
PLASMA SPRAYED POROUS ZIRCONIA

LIGHT REGIONS = ZrO_2
DARK REGIONS = POROSITY

TYPICAL MORPHOLOGY — SURFACE VIEW
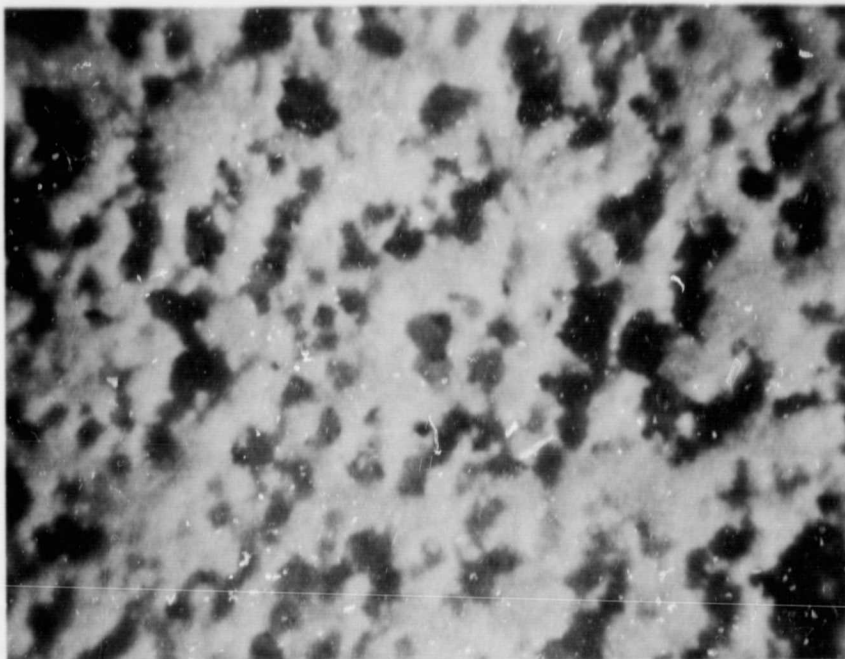
200µm

UTRC NO. 80-95 POROUS ZIRCONIA — CROSS SECTIONAL VIEW

100µm

81-8-92-19

FIG. 3-6
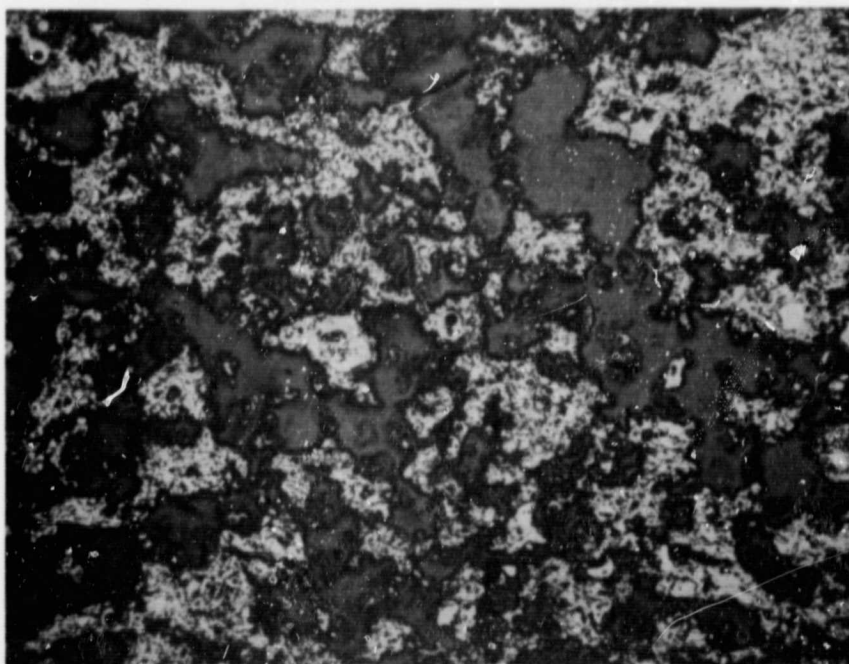
PLASMA SPRAYED MICROCRACKED ZIRCONIA
UTRC NO. 80-96

BRANCHING

RADIAL MICROCRACKS

200μm

81-8-92-20

18

FIG. 3-7
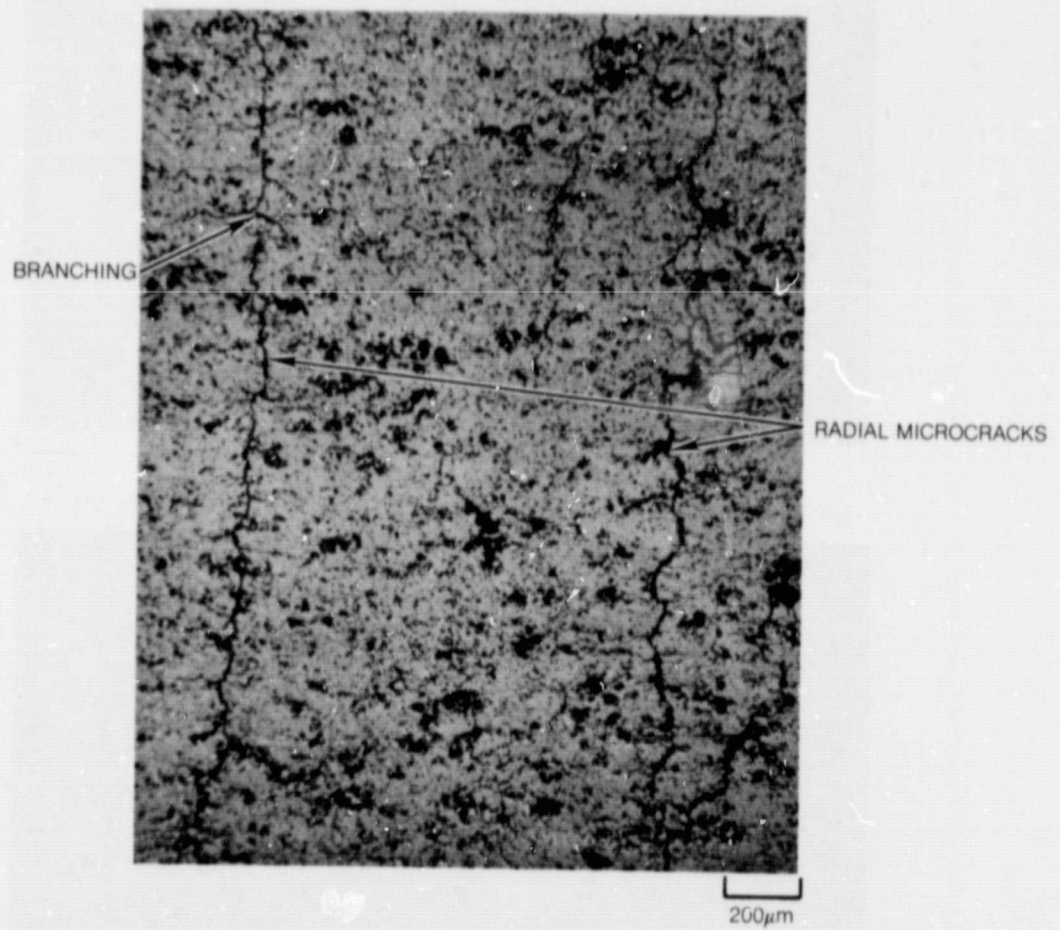
PLASMA SPRAYED LOOSELY BOUND ZiRCONIA
UTRC NO. 80-98

NOTE SPLAT OUTLINES OF ZIRCONIA PARTICLES

100μm

81-8-92-18

FIG. 3-8
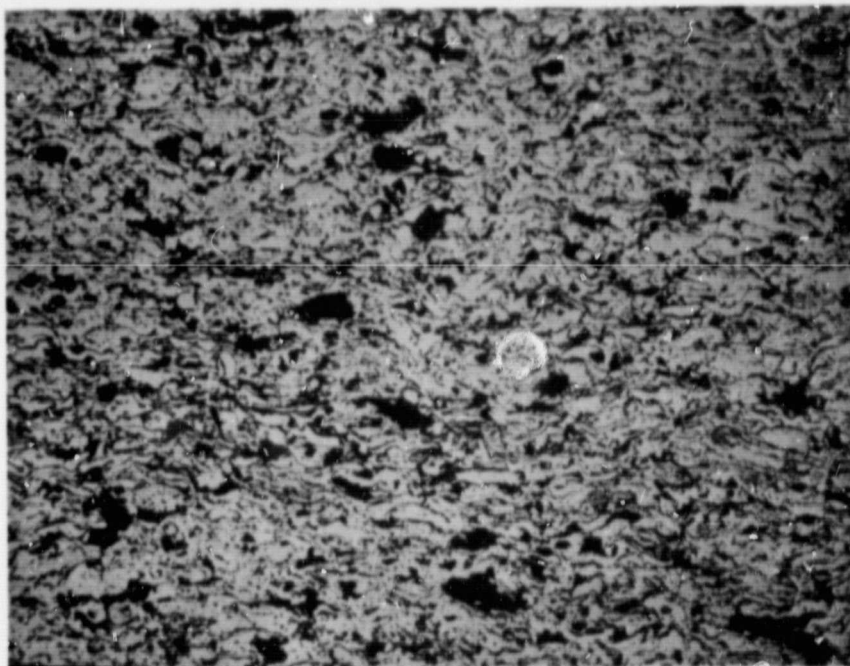
FOUR POINT BEND PROPERTIES OF LOW MODULUS ZIRCONIA SPECIMENS
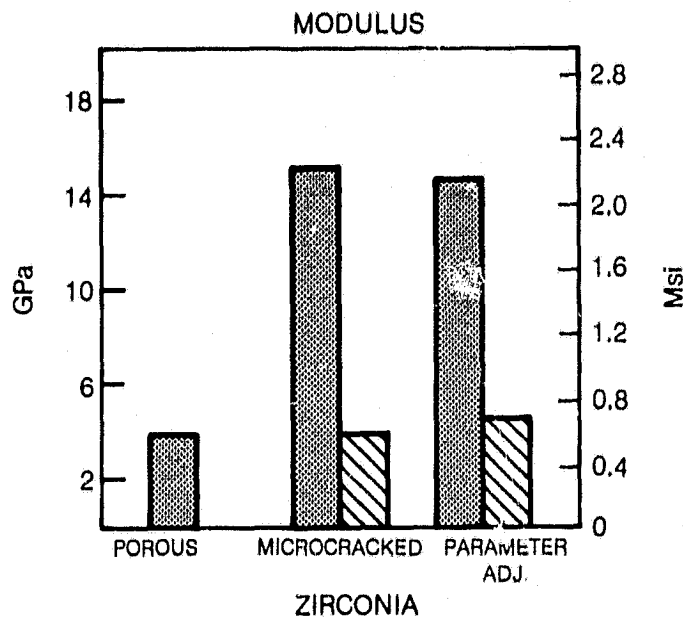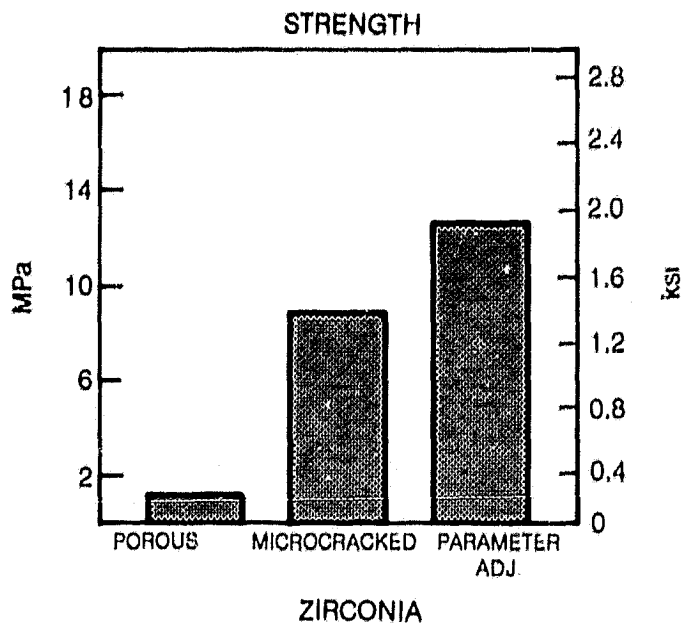
IV. TASK III - EVALUATION OF CANDIDATE SYSTEMS

Figure 4-1 summarizes the systems selected in Task II for evaluation in Task III. For Task III, a coarser fraction of NiCrAlY was selected in an effort to reduce oxidation. For this effort, -100 + 200 mesh NiCrAlY was chosen and used throughout the remainder of the program. Evaluation in Task III consisted of the following testing.

- Measurement of strength and modulus at room temperature and at 1089°K. This was accomplished both in the as fabricated condition and after aging at 1311°K for 500 hours.

- Static oxidation at 1311°K for periods of 1, 10, 100, 200, and 500 hours. Weight and dimensional changes were monitored for each interval.

- Cyclic oxidation between room temperature and 1311°K. Each cycle consisted of 65 minutes at 1900°F and 15 minutes at room temperature. Weight and dimensional changes were recorded after 1, 10, 50 and 100 cycles.

- Thermal conductivity. Measurements were made in the thickness direction at temperatures between room temperature and 1116°K. Measurements were made by Purdue University.

- Attachment. Demonstration was accomplished by attaching each system to both a 304 SS substrate and to a Haynes-25 substrate.

- Optical microscopy. Photomicrographs were obtained to examine the as fabricated state of each system and the effect of thermal aging.

4.1 Mechanical, Oxidation, and Thermal Tests

4.1.1 Results

Figure 4-2 compares strength and modulus values of the three systems in the as fabricated and aged 500 hours at 1311°K conditions. The data are presented in Tables A-8, A-9, A-10, A-11, A-12 and A-13. For the Brunsbond[R] Pad, failure occurred within the gage length of the extensometer, indicating that the tapered doublers were an improvement over the non-tapered configuration of Task II.

Figure 4-3 compares static and cyclic oxidation of the three systems. Dimension changes and oxidation data are presented in Tables A-14, A-15, A-16, A-17, A-18 and A-19.

Figures 4-4, 4-5 and 4-6 compare specific heat, thermal diffusivity, and thermal conductivity as functions of temperature for the three systems. The data are presented in Tables A-20, A-21 and A-22. This work was performed by R. E. Taylor and H. Groot, TPRL 249, Thermophysical Properties Research Laboratory, School of Mechanical Engineering, Purdue University, West Lafayette, Indiana.

4.1.2 Discussion

4.1.2.1 35% Dense Brunsbond[R] Pad

1. Modulus remains between 10.3 and 3.45 GPa (1.5 and 0.5 MSI) at temperatures between RT and 1089°K. This is true even after extensive exposure to severe static oxidation conditions (500 hours @ 1311°K), as shown in Fig. 4-2.

2. Questions arise concerning the high temperature structural behavior. Linear extrapolation of the two strength values (Fig. 4-2) indicates that the strength goes to a low value at the upper temperature range of interest (1255-1311°K). While an extrapolation must be recognized for what it is, the high temperature strength of Brunsbond[R] Pad should be examined further.

   In particular, the following questions should be addressed:

   . What is the relationship between strength of the fiber pad and Hoskins 875 alloy from which the fibers are fabricated? Is the fiber pad strength simply a ratio of the alloy strength?

   . What is the low cycle fatigue behavior as a function of temperature?

   . How does entanglement of the fibers affect the measured strength, especially at high temperature?

   . What are the high temperature creep properties of the material? If the creep resistance is low, the pad may truly be a strain isolator under steady state conditions.

   . What is the effect of crosshead speed on property measurements? Data presented here was obtained at 0.254 mm/min strain rate. Literature data (Ref. 7) gives a 1089°K strength of 1000 psi for 35% dense Brunsbond[R] Pad which was produced at a crosshead speed of 5.09 mm/min (Ref. 8).

3. Static and cyclic oxidation (summarized in Fig. 4-3) show comparable weight and dimensional changes. A total of + 1.3% increase in weight occurred after 500 hours at 1311°K in static oxidation and no more than one percent dimensional change occurred under these conditions.

4. Thermal conductivity ranges from $\sim$ 0.01 W cm^{-1}K^{-1} at room temperature to 0.026 W cm^{-1}K^{-1} at 1116°K. The peak in the specific heat versus temperature curve at $\sim$ 800°K is associated with the Curie point. Specimens used for this test were .254 cm thick and brazed (by Brunswick) to a stainless steel substrate. Thickness of the fiber metal might have an effect on the measured thermal conductivity value. This could occur due to heat transmission through the Brunsbond^R Pad by radiation since the pad is of low density and thin specimens are optically transparent in part.

5. Microstructurally (Fig. 4-7), strength at room and elevated temperature appears to be due to the amount of bridging between the fibers and the fiber entanglement. Oxidation is limited to oxide formation at the fiber surface (Fig. 4-8). No internal oxidation is indicated after 500 hours at 1900°F since porosity within the fibers is absent. Brunsbond^R Pad at 35% density has a potential life of 1000 hours at 1311°K.

4.1.2.2 Porous NiCrAlY

1. Modulus of the as-fabricated material (Fig. 4-2) is between 9.6 and 6.9 GPa (1.4 and 1.0 MSI) between room temperature and 1089°K. After static oxidation for 500 hours at 1311°K, the modulus is 23.4 to 18.6 GPa (3.4 to 2.7 MSI) between room temperature and 1089°K.

   The increase in modulus with thermal aging is probably due to sintering and the conversion of metal to oxide.

2. As-fabricated strength is 26.1 to 18.6 MPa (3.8 to 2.7 KSI) between room temperature and 1089°K. Aged strength is 48.2 to 20.0 MPa (7.0 to 5.8 KSI) between room temperature and 1089°K. The increase in strength with thermal aging is consistent with the sintering and formation of oxide products.

3. Static and cyclic oxidation produce similar results. Static oxidation, Fig. 4-3, after 500 hours at 1311°K gives a weight gain of + 10.5%. There is less than +2% change in dimension after 500 hours at 1311°K. The measured weight gains with oxidation are consistent with a high specific surface area plasma sprayed metal. Dimensional changes due to oxidation could give rise to stresses at the ceramic-porous NiCrAlY interface and this could limit the high temperature use.

   Oxidation can cause problems because conversion of NiCrAlY metal to oxides should occur at the ceramic NiCrAlY interface. This is likely because of the temperature at this position and the high oxygen potential especially with a zirconia layer due to its oxygen ion conduction capability. Spalling of the oxide scale could occur due to thermal cycling leading to failure of the system along the interface. Means to limit oxide formation at the interfacial region should be investigated and could include the following:

. Vapor deposition of a protective coating.

. Argon atmosphere spraying of the NiCrAlY to promote metallurgical bonding between the splats to decrease effective surface area.

. Oxidation of the sprayed layer prior to ceramic deposition.

4. Thermal conductivity, Figs. 4-4, 4-5, & 4-6, ranges from $\sim$ 0.007 W cm^{-1}K^{-1} at room temperature to $\sim$ 0.02 W cm^{-1}K^{-1} at 1116°K.

5. Microstructurally (Fig. 4-9), plasma sprayed porous NiCrAlY has a very high surface area. This produces high measured oxidation values due to the formation of oxides around each splat (Fig. 4-10). Means to reduce oxidation should be centered around reducing the specific surface area or reducing exposure to temperature. Oxide formation should produce a decrease in the coefficient of thermal expansion which may offset an increase in modulus. Since oxidation occurs primarily in the hottest region of the low modulus interlayer, i.e., along the ZrO_2/NiCrAlY interface, the cooler region should maintain its modulus.

4.1.2.3 Microcracked Zirconia

1. Modulus, Fig. 4-2, is 6.2 to 3.4 GPa (.9 to .5 MSI) between room temperature and 1089°K for the as-fabricated condition, and from 17.2 to 10.3 GPa (2.5 to 1.5 MSI) in the aged condition for that temperature range.

2. Strength measurements show 9.6 to 11.7 MPa (1.4 KSI to 1.7 KSI) between 70 to 1089°K for the as-fabricated condition and 11.0 to 14.5 MPa (1.6 to 2.1 KSI) for the aged.

3. Oxidation testing, Fig. 4-3, shows that no significant weight or dimensional change occurred.

4. Thermal conductivity, Fig. 4-6, remains almost constant at 0.01 W cm^{-1}K^{-1} between room temperature and 1116°K.

5. Microstructurally (Fig. 3-6) zirconia has radial microcracks which exhibit a high degree of branching in the X-Y plane.

Thermal cycling of a free standing body of microcracked zirconia does not appear to link up the microcracks, Fig. 4-11. However, the behavior of the system under constraint is unknown. For this reason, it is necessary to conduct thermal cycling of the microcracked zirconia in a strain isolator seal configuration to properly evaluate it. Preferably a cyclic thermal gradient would be imposed but even a constant temperature thermal cycle would provide useful information.

24

4.2 Attachment Demonstration

Each of the systems was fabricated onto stainless steel and Haynes 25 alloy substrates. The Brunsbond[R] Pad was attached by use of a brazing operation. The microcracked zirconia and porous NiCrAlY were plasma sprayed directly onto Metco 443 bondcoated substrate surfaces. Specimens of each of these systems attached to both types of substrates were delivered to the NASA Program Manger, R. C. Bill.

4.3 Selection of Task IV Candidate Material

Each Task III candidate material offers attractive properties that warrant further testing.

The porous NiCrAlY system was selected for further evaluation in Task IV, based on discussions between UTRC and the NASA Program Manager. The NiCrAlY system can be used in any situation that the zirconia system can be used, and may offer fabrication advantages over the fiber metal approach.

The as-fabricated properties of porous NiCrAlY are desirable, however, the modulus increases with oxidation exposure. The amount of oxidation per time is largely due to the high specific surface area of the sprayed NiCrAlY. Efforts to decrease oxidation were made in Task II in switching from a -170 + 325 mesh to a -100 + 200 mesh powder. This produced roughly half the measured oxidation. A further increase in size is not practical from a spraying point of view.

In order to offset the increase in modulus with aging, a lower density (and therefore, lower modulus) NiCrAlY system was selected for evaluation in Task IV.

FIG. 4-1

TASK II SELECTED CANDIDATES AND TASK III EVALUATION

TASK II

35% BRUNSBOND PAD   2870 Kg/M^3 MICROCRACKED
                            NiCrAlY   ZIRCONIA

TASK III EVALUATION

MODULUS
STRENGTH
OXIDATION
THERMAL CONDUCTIVITY
MICROSTRUCTURE

TASK IV SELECTION

81—8—92—5

26

FIG. 4-2
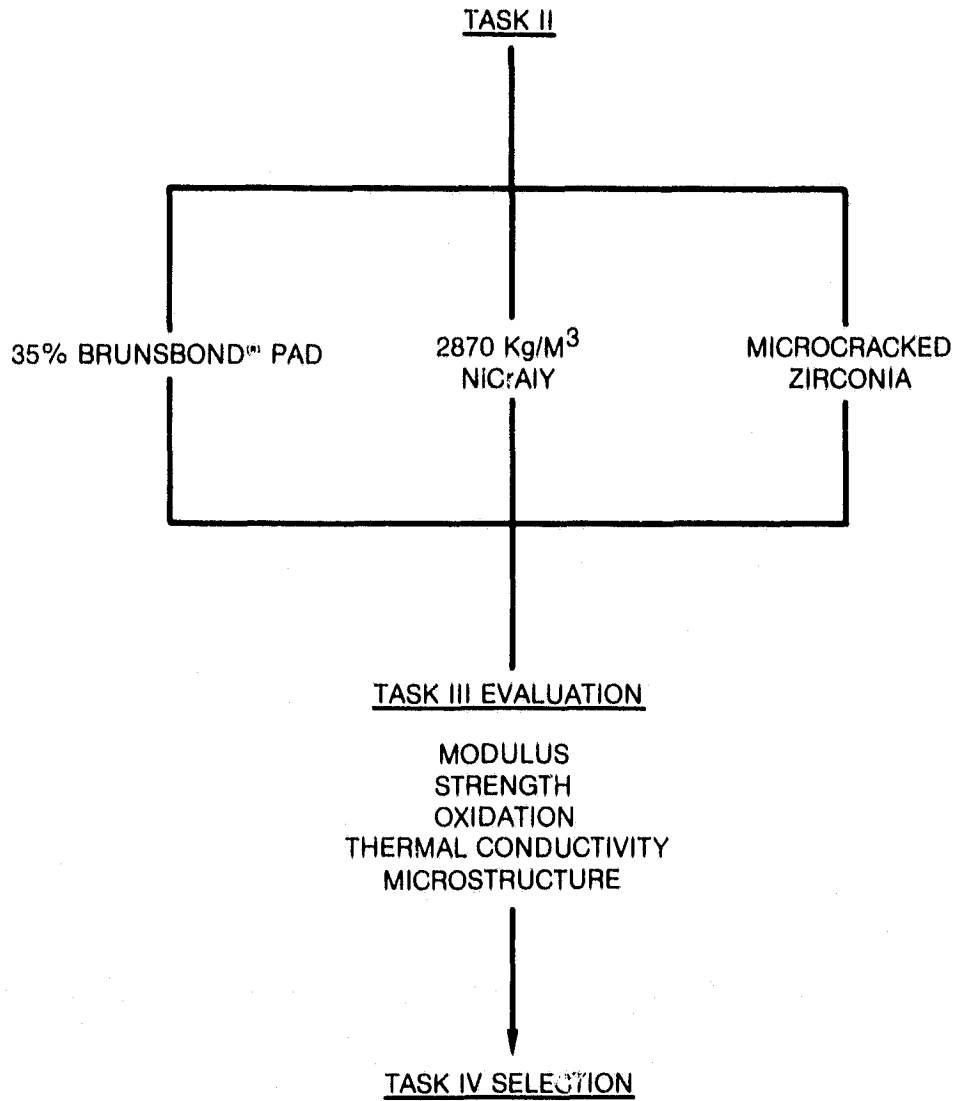
TASK III — SPECIMEN PROPERTIES

STRENGTH

△ = ZIRCONIA
○ = FIBERMETAL
□ = NiCrAlY

AS-FABRICATED

AGED 500 hrs AT 1310°K
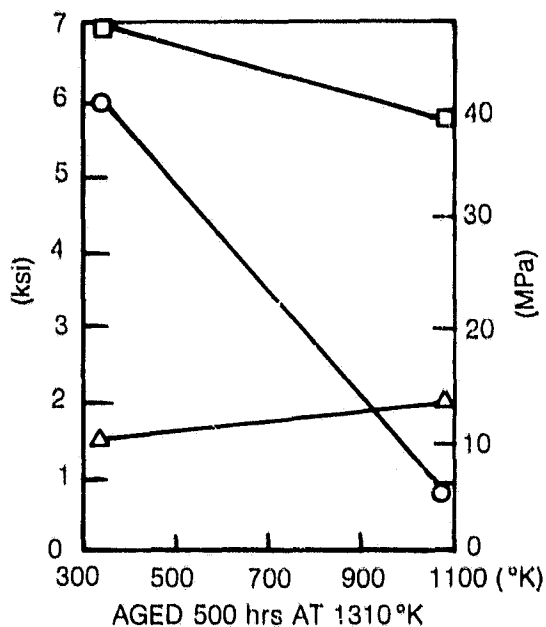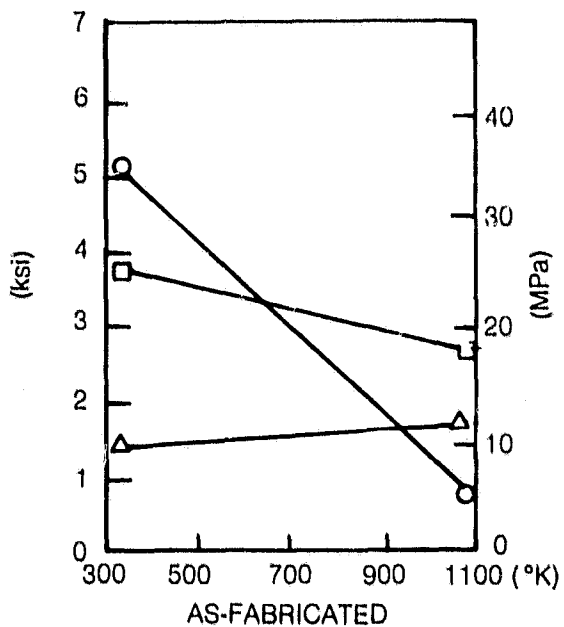
MODULUS

□ = OPEN = STRAIN GAGE
■ = BLACKENED = DEFLECTOMETER, ETC

AS-FABRICATED

AGED 500 hrs AT 1310°K

81—4—36—2

27
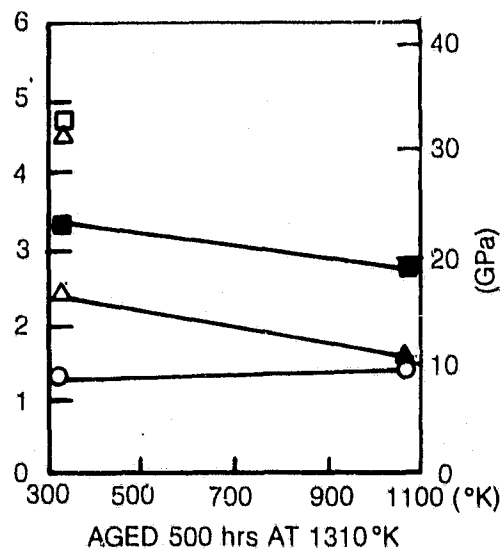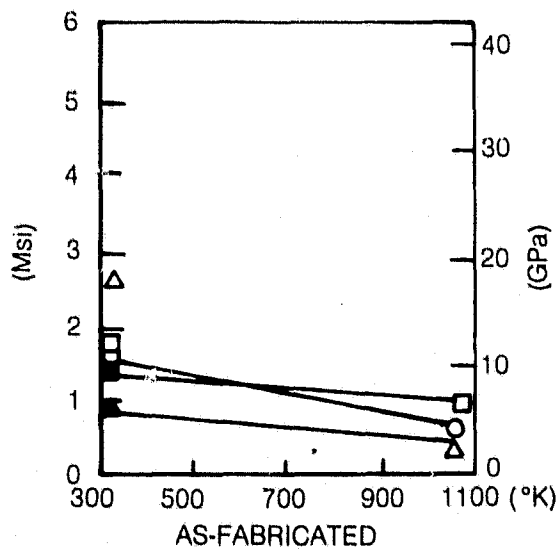
TASK III — SPECIMEN OXIDATION

Δ — ZIRCONIA
O — FIBERMETAL
□ — NiCrAlY

CYCLIC OXIDATION 295°K TO 1310°K

STATIC OXIDATION AT 1310°K

FIG. 4-3

81-4-36-3

28

FIG. 4-4

SPECIFIC HEAT OF TASK III CANDIDATES
(FROM TPRL 249, TAYLOR & GROOT)

FIG. 4-5

THERMAL DIFFUSIVITY OF TASK III CANDIDATES
(FROM TPRL 249, TAYLOR & GROOT)

FIG. 4-6

THERMAL CONDUCTIVITY OF TASK III CANDIDATES
(FROM TPRL 249, TAYLOR & GROOT)

FIG. 4-7
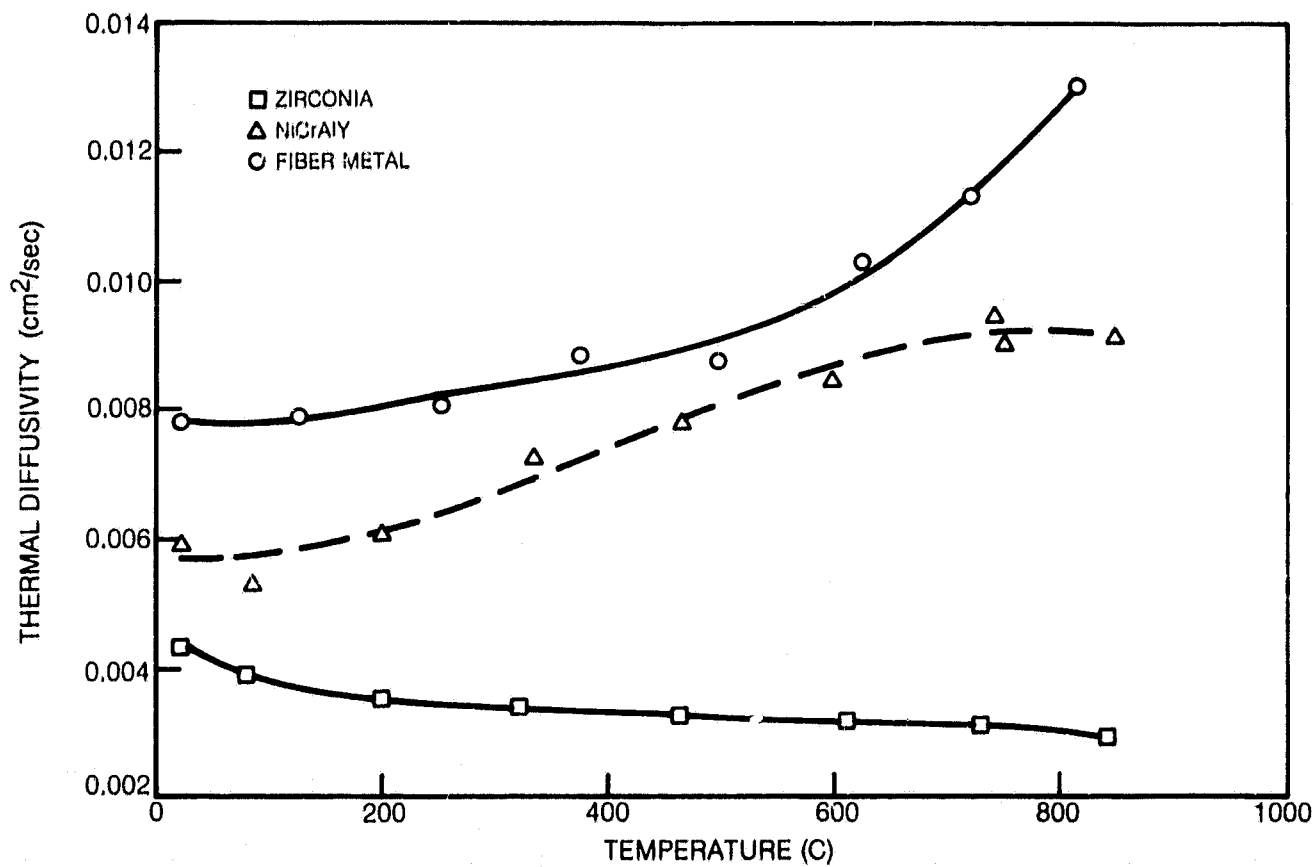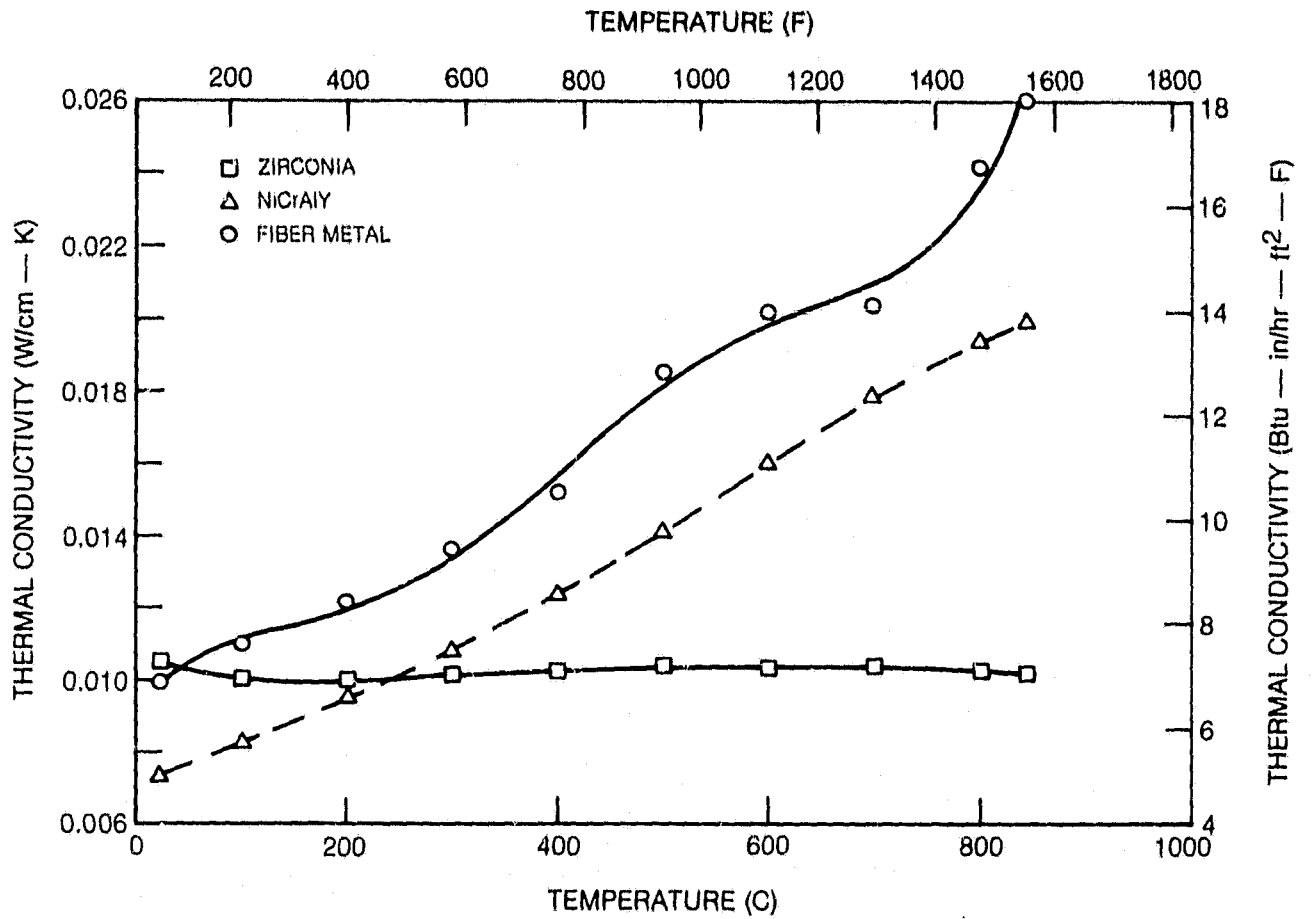
35% DENSE BRUNSBOND® PAD

SURFACE VIEW SHOWING FIBER ENTANGLEMENT

700μm
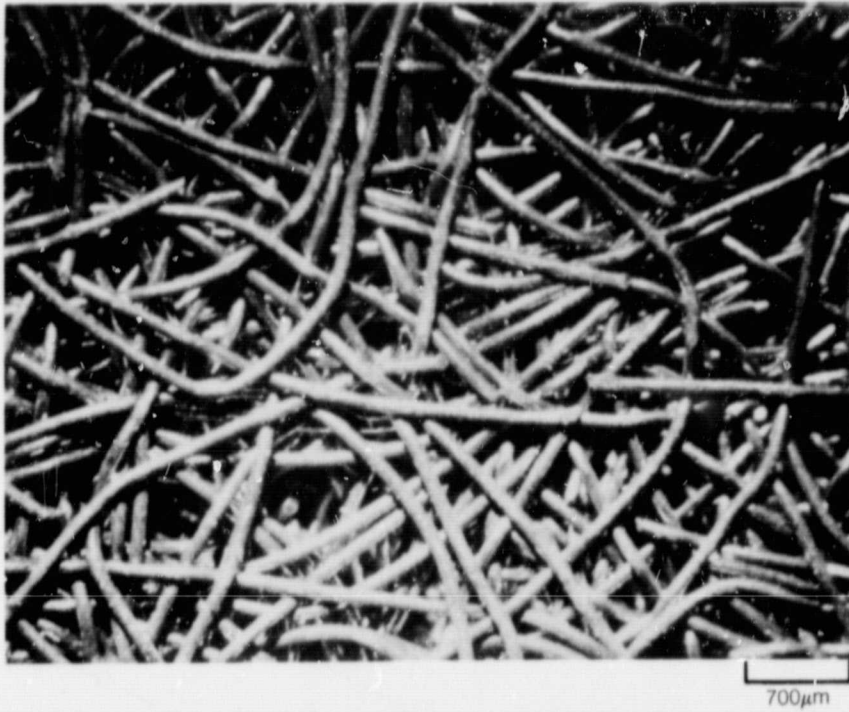
CROSS SECTIONAL VIEW SHOWING BRIDGING BETWEEN FIBERS

SINTERED BRIDGES
BETWEN FIBERS

100μm

81-8-92-17

FIG. 4-8
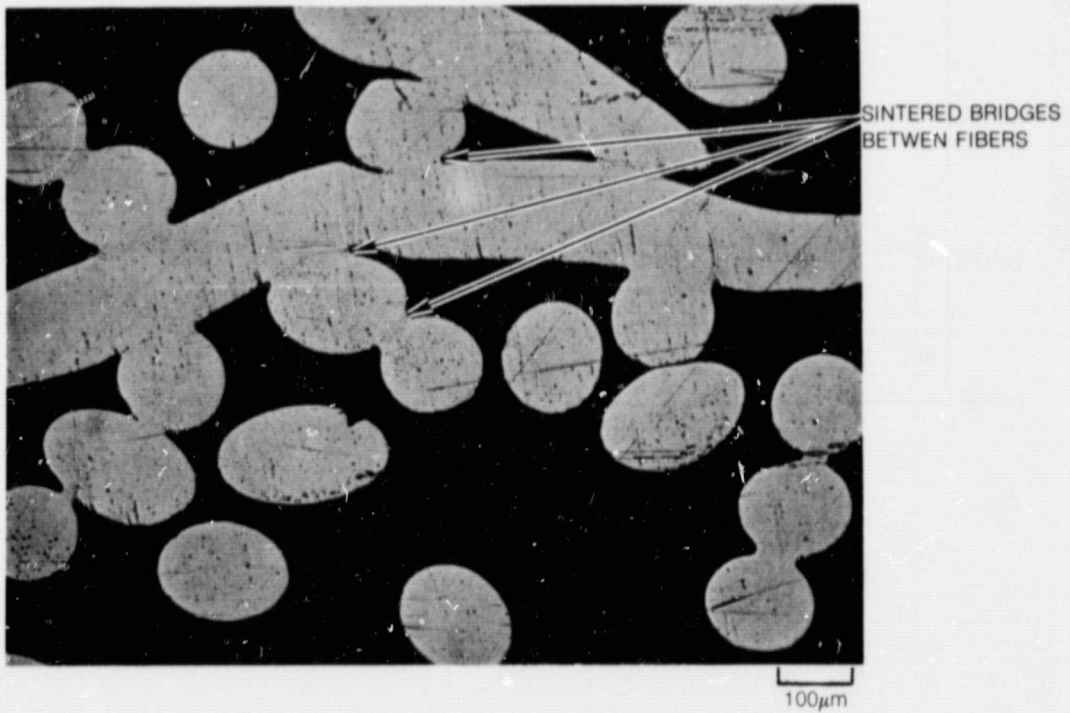
OXIDATION OF BRUNSBOND® PAD

AS RECIEVED
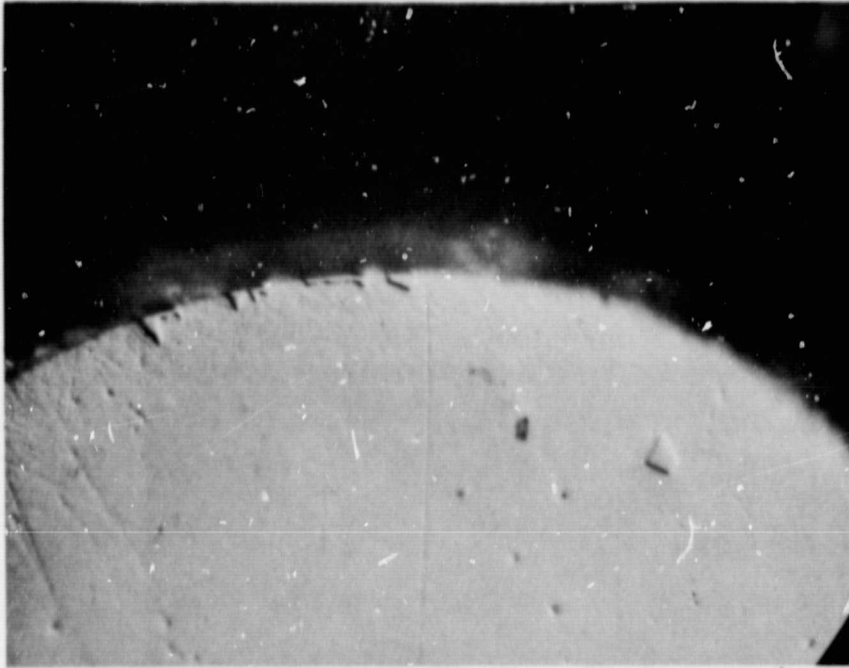
SMOOTH WIRE SURFACE IN AS
FABRICATED CONDITION

10μm

500 hr AT 1311°K
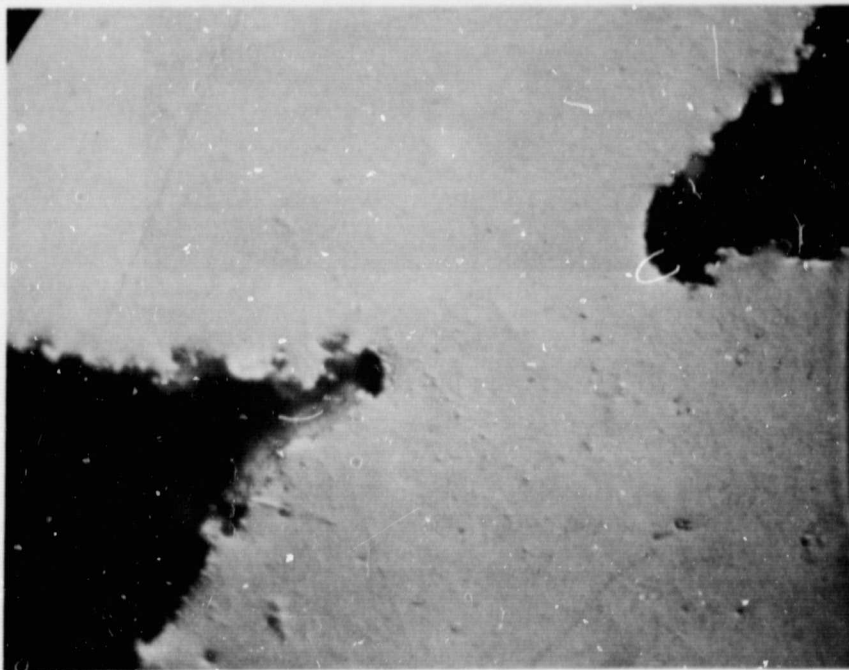
SURFACE OXIDATION

10μm

81-8-92-16

33

FIG. 4-9

PLASMA SPRAYED POROUS NiCrAlY
UTRC NO. 81-16, DENSITY = 3010 Kg/M^3

LIGHT AREAS = NiCrAlY
DARK AREAS = POROSITY

PLASMA SPRAYED POROUS NiCrAlY EXHIBITS HIGH SPECIFIC SURFACE AREA

SPRAY DIRECTION

100μm

81—8—92—15

FIG. 4-10
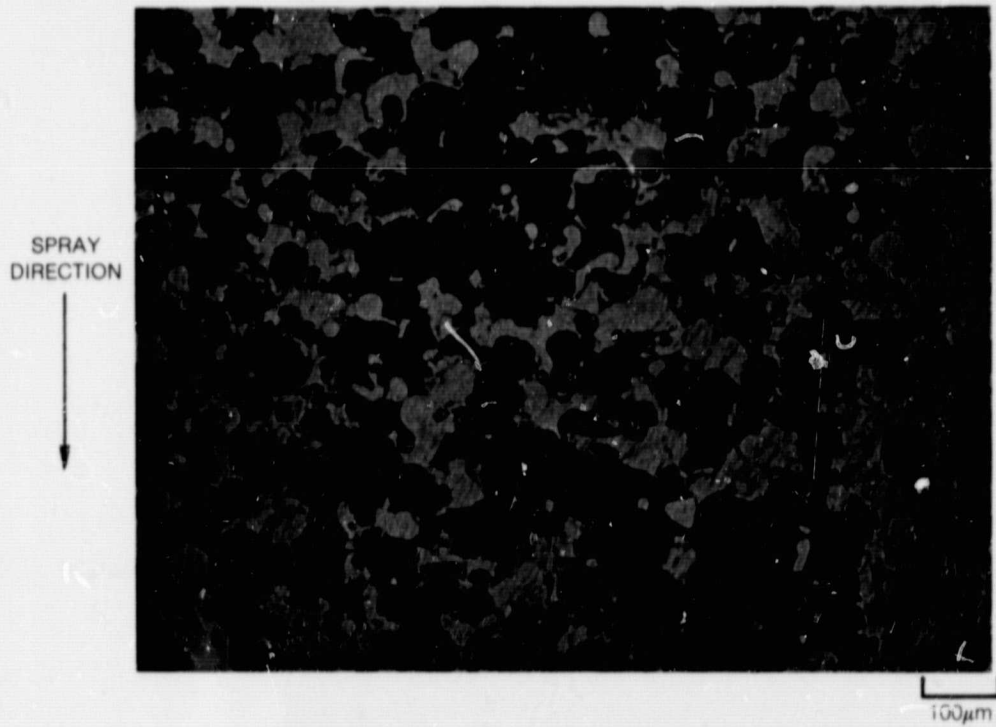
PLASMA SPRAYED POROUS NiCrAlY — TASK III
OXIDE FORMATION ON THERMAL AGING

NiCrAlY

UTRC 81-016 AS SPRAYED

10μm

OXIDE

NiCrAlY

UTRC 81-016 AGED 500 hr AT 1311°K

20μm

81-8-92-23

FIG. 4-11

MICROCRACKED ZIRCONIA AFTER THERMAL CYCLING
UTRC NO. 80-129

MICROCRACKS DO NOT APPEAR TO LINK UP DUE TO THERMAL CYCLING

50μm

81-8-92-13
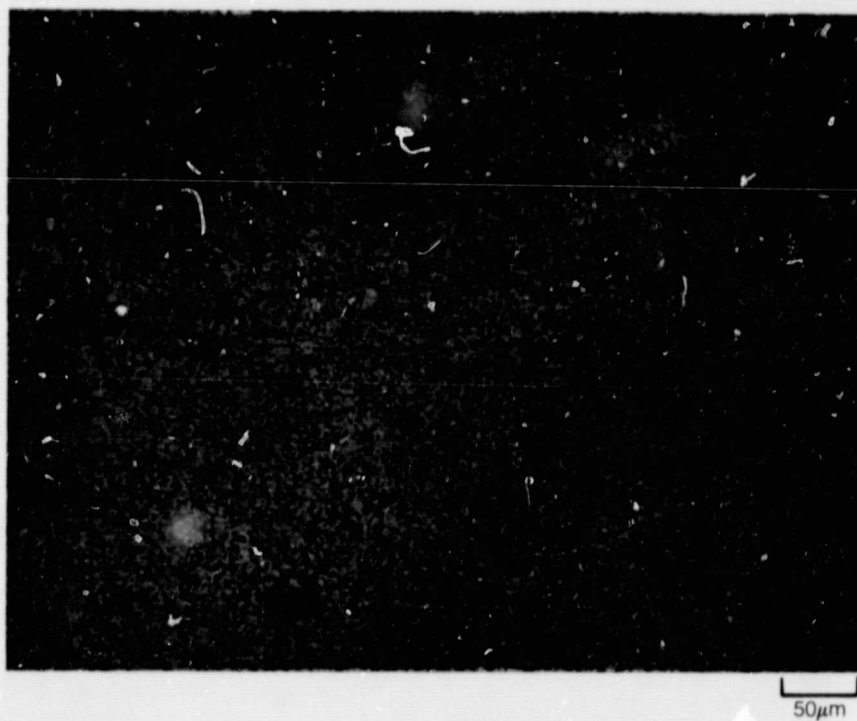
V. TASK IV - OPTIMIZATION AND EVALUATION OF A SELECTED CANDIDATE SYSTEM

Porous NiCrAlY was chosen for further optimization in Task IV based on discussions between the Research Center and NASA Program Manager.

Task III data showed that the modulus of the porous NiCrAlY (density 3010 kg/M^3) increased substantially with thermal aging. The room temperature modulus went from 9.7 GPa (1.4 MSI) to 23.5 GPa (3.4 MSI). At 1089°K the modulus increased similarly. This large increase in undesirable because it tends to defeat the concept of the low modulus strain isolator system.

Any technique limiting the amount of oxidation in the porous NiCrAlY would have a beneficial effect on maintaining the as-sprayed modulus. Decreasing the specific surface area of the structure is important and was achieved in Task III by using a more coarse fraction (-100 + 200 mesh) of NiCrAlY powder than in Task II (-170 + 325 mesh). The result was an approximate halving of the measured oxidation. Further increase in the powder size was not examined because it would probably decrease the efficiency of the spray fabrication process. Other possible means to effectively reduce the specific surface area (e.g., sputtering a protective coating or use of an argon spray atmosphere to promote metallurgical bonding) were not within the scope of this program.

The approach evaluated in Task IV to maintain an acceptable modulus in the porous NiCrAlY, involved starting with a lower modulus system. Specimens of porous NiCrAlY, density 2347 kg/M^3, were prepared from -100 + 200 NiCrAlY powder and Metco 600 polyester. The as-fabricated modulus was 2.96 GPa (.43 MSI) compared with 9.7 GPa (1.4 MSI) in Task III. With oxidation, the modulus would increase but to a lower value than that obtained with the Task III system.

5.1 Mechanical, Oxidation, and Thermal Tests

5.1.1 Results

Figure 5-1 shows strength and modulus of the 2347 kg/M^3 porous NiCrAlY at room temperature and 1089°K in the as-sprayed and aged conditions. The data are presented in Tables A-23 and A-24.

Figure 5-2 shows static and cyclic oxidation. The dimension change and oxidation data are presented in Tables A-25 and A-26.

Figures 5-3, 5-4 and 5-5 show specific heat, thermal diffusivity, and thermal conductivity as functions of temperature for both the Task IV and Task III NiCrAlY systems. The data are presented in Tables A-27, A-28 and A-29. This work was performed by R. E. Taylor and H. Groot, TPRL 249A, Thermophysical Properties Research Laboratory, School of Mechanical Engineering, Purdue University, West Lafayette, IN.

5.1.2 Discussion

a. The modulus is between 2.96 and 1.77 GPa (0.43 and 0.26 MSI) for the as-fabricated condition between room temperature and 1089°K. After aging 500 hours at 1311°K, the modulus is between 11.8 and 11.5 GPa (1.71 and 1.67 MSI) for the same temperature range. This represents a substantial improvement over the Task III porous NiCrAlY which exhibited an aged modulus range of 23.3 to 19.0 GPa (3.4 to 2.8 MSI).

b. The strength is between 11.2 and 8.05 MPa (1.6 and 1.2 KSI) for the as-fabricated condition between room temperature and 1089°K. After aging 500 hours at 1311°K, the strength is between 20.4 and 12.2 MPa (2.97 and 1.78 KSI). Compared with the Task III NiCrAlY (strength 26.4 to 18.6 MPa as-sprayed and 48.3 to 39.8 MPa aged), the strength of the Task IV NiCrAlY has been reduced by the effort to preserve a desirable modulus in the aged condition. The decrease in strength is consistent with a lower density system.

c. Static and cyclic oxidation summarized in Fig. 5-2 show similar effects of high specific surface area due to the high porosity of the Task IV NiCrAlY. After 500 hours at 1311°K, static oxidation results showed a 16% weight increase.

Calculations based on Ni-25Cr-6Al-.35Y indicate that a percent weight gain of about 17% would consume all the chromium, aluminum, and yttrium (assuming preferential oxidation of these elements and that Cr_2O_3, Al_2O_3, and Y_2O_3 are formed). The calculation is complicated by the different splat sizes present in the NiCrAlY structure such that nickel in the small splats would be consumed long before nickel in the large splats. However, an oxidation weight gain of +16% after 500 hours at 1311°K indicates that the fine structures within the NiCrAlY material probably have been converted totally to oxides while only the medium to large structures still exhibit a metallic phase. This is apparent in the microstructure (Fig. 5-6).

d. Thermal conductivity of the Task IV NiCrAlY compared to the Task III NiCrAlY is related to the square of the ratio of the densities of the two. This can be seen from the following points: (1) the specific heat values are the same for the two specimens indicating that the material composition is the same; (2) the thermal diffusivity values of the Task IV NiCrAlY are reduced approximately by the ratio of the densities of the two systems; (3) finally, the conductivity is calculated by the formula $K = C_p \alpha d$ where K is the conductivity, C_p is the specific heat, α is the thermal diffusivity, and d is the density. Thus, the ratio of conductivities is related to the square of the ratio of densities. This fact is important because it indicates the dependency of conductivity on density for systems

38

at these levels. It may be possible to use this effect to advantage in the design of the system since a thin porous NiCrAlY layer of higher density at the interface with the ceramic should have improved oxidation resistance.

e. Microstructurally (Fig. 5-7), the Task IV NiCrAlY is similar to the Task III NiCrAlY but has a slightly lower density of metal.

5.2 Attachment Demonstration

The Task IV porous NiCrAlY, density 2347 kg/M^3, was sprayed onto Haynes 25 alloy to demonstrate attachment. A Metco 443 bondcoat was used between the substrate and NiCrAlY strain isolator. A specimen of this system was delivered to the NASA Program Manager.

FIG. 5-1

STRENGTH AND MODULUS OF 2347 Kg/M³ POROUS NICrAIY
AT 295° AND 1310°F AS-SPRAYED AND AGED

OPEN-STRAIN GAGE, EXTENSOMETER
BLACKENED-DEFLECTOMETER

81-8-92-24

FIG. 5-2
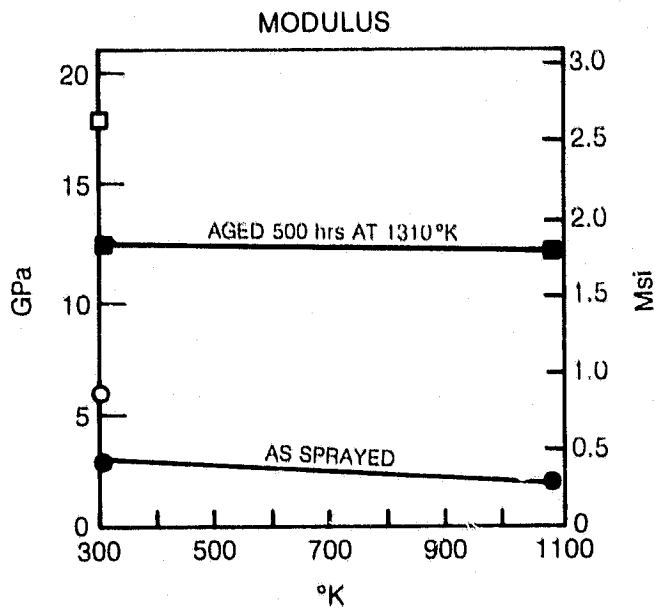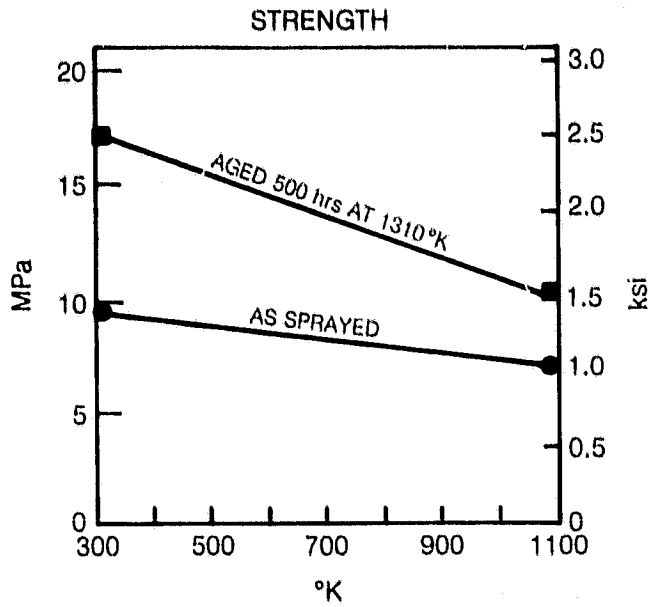
TASK IV NiCrAlY OXIDATION
DENSITY 2347 Kg/M³

STATIC OXIDATION AT 1311°K
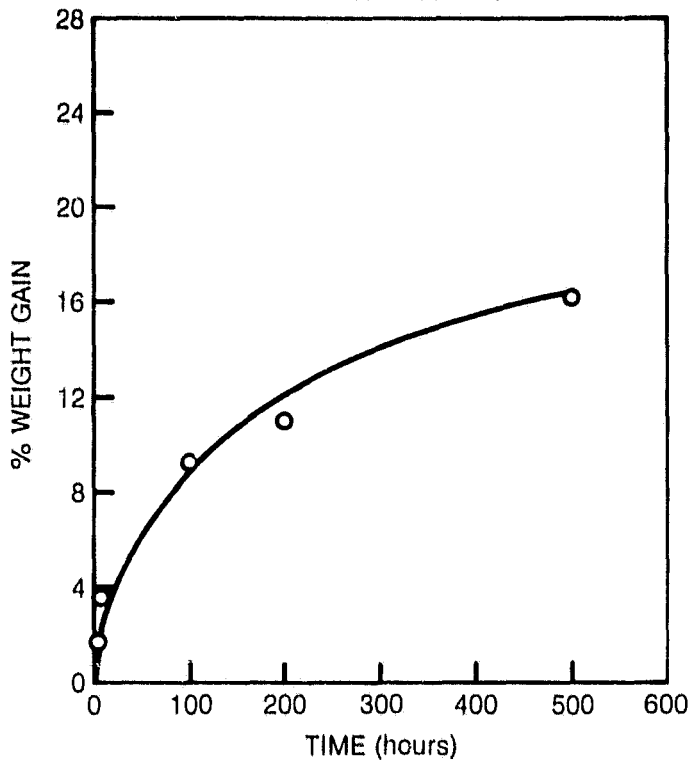
CYCLIC OXIDATION 293°K TO 1311°K

81-8-92-4

41

FIG. 5-3
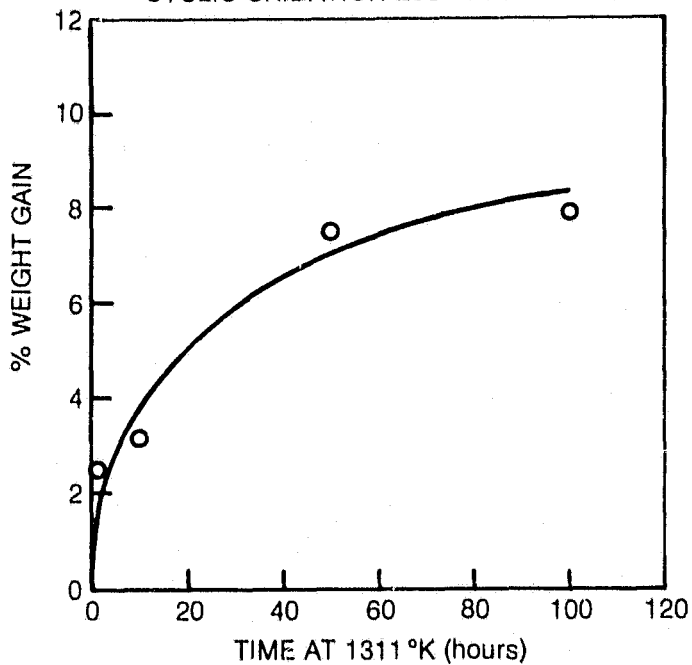
TASK IV NICrAIY — SPECIFIC HEAT
(FROM TPRL 249A, TAYLOR & GROOT)

81—8—92—10

FIG. 5-4
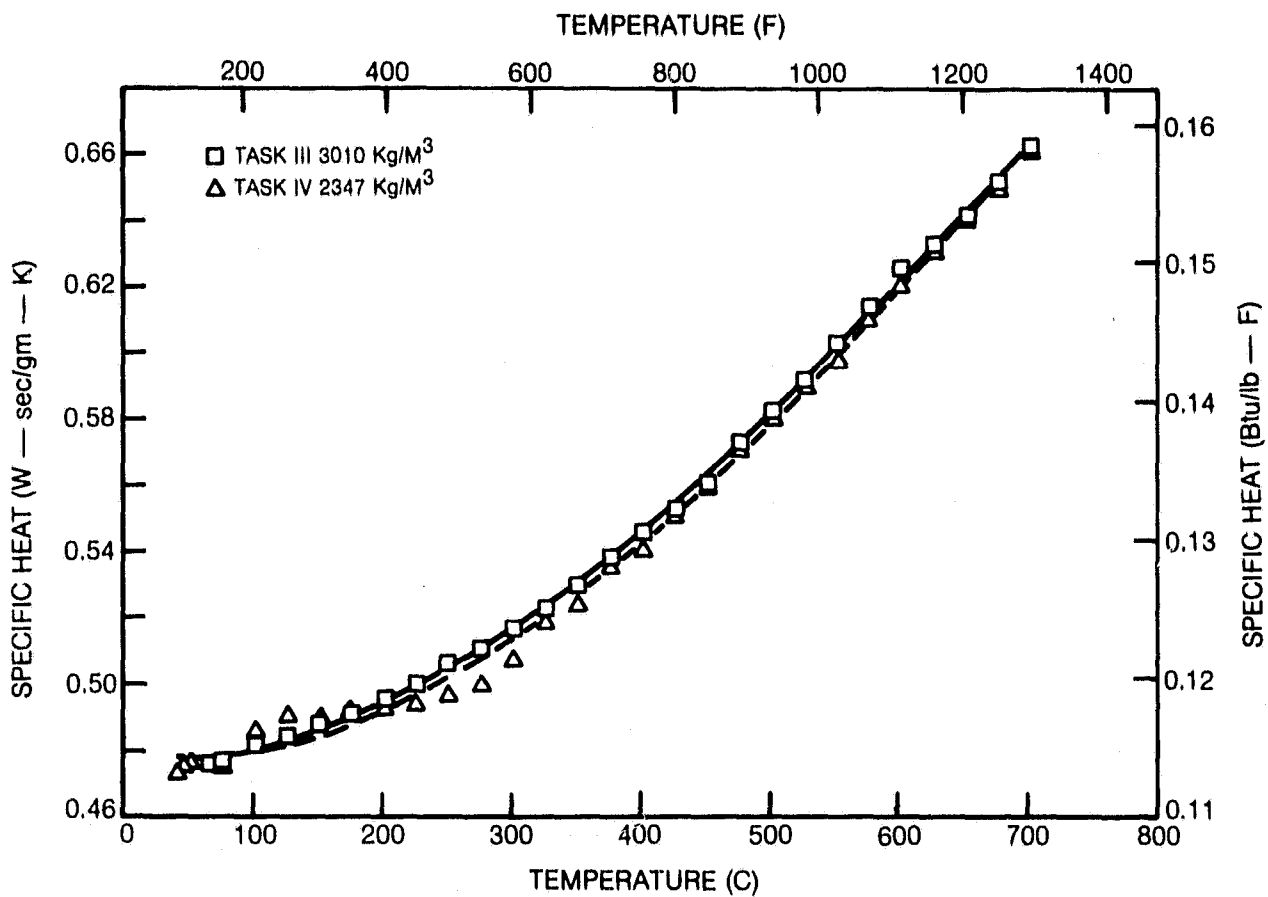
TASK IV NiCrAIY — THERMAL DIFFUSIVITY
(FROM TPRL 249A, TAYLOR & GROOT)

81—8—92—9

FIG. 5-5
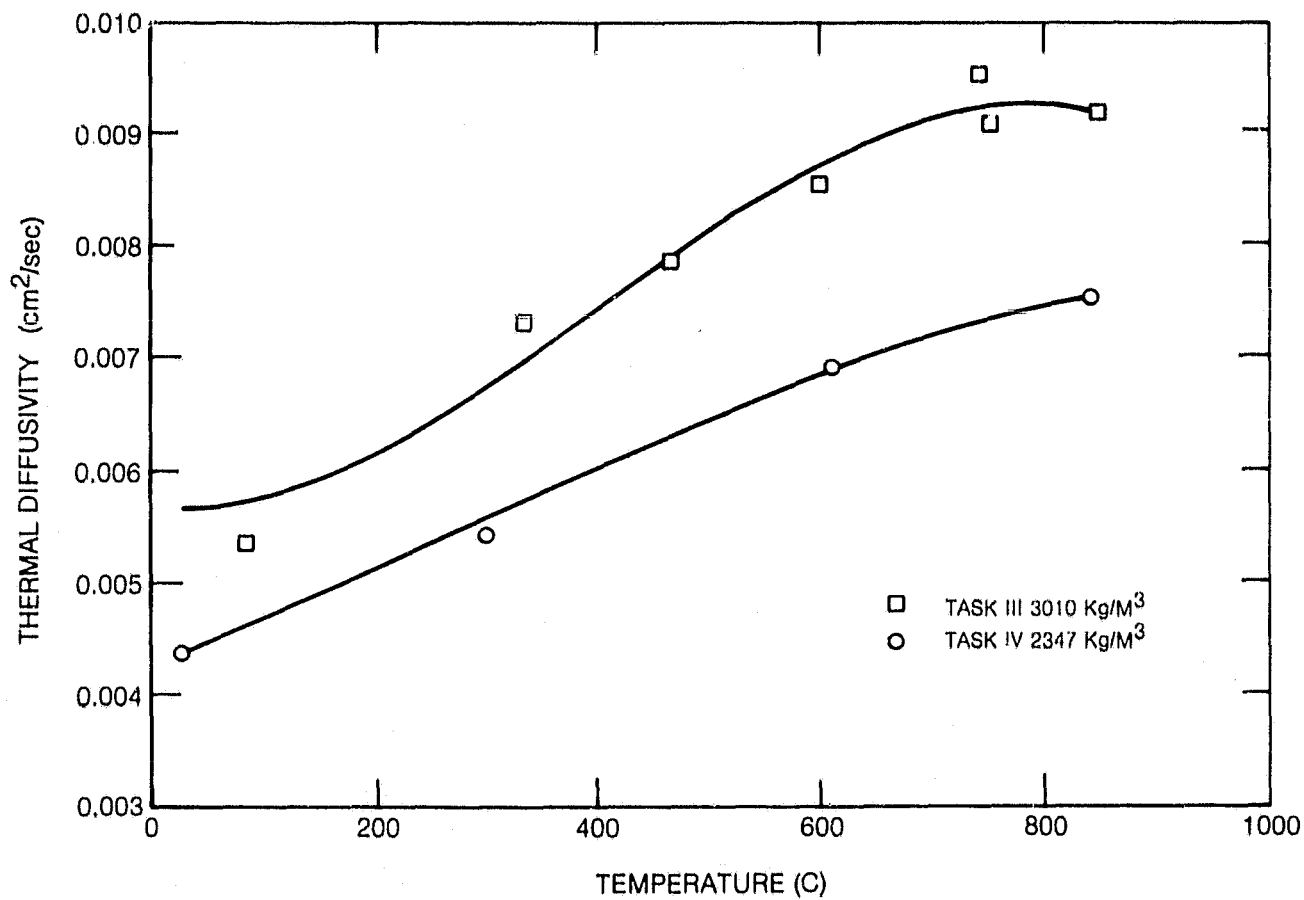
TASK IV NiCrAlY — THERMAL CONDUCTIVITY
(FROM TPRL 249A, TAYLOR & GROOT)

FIG. 5-6
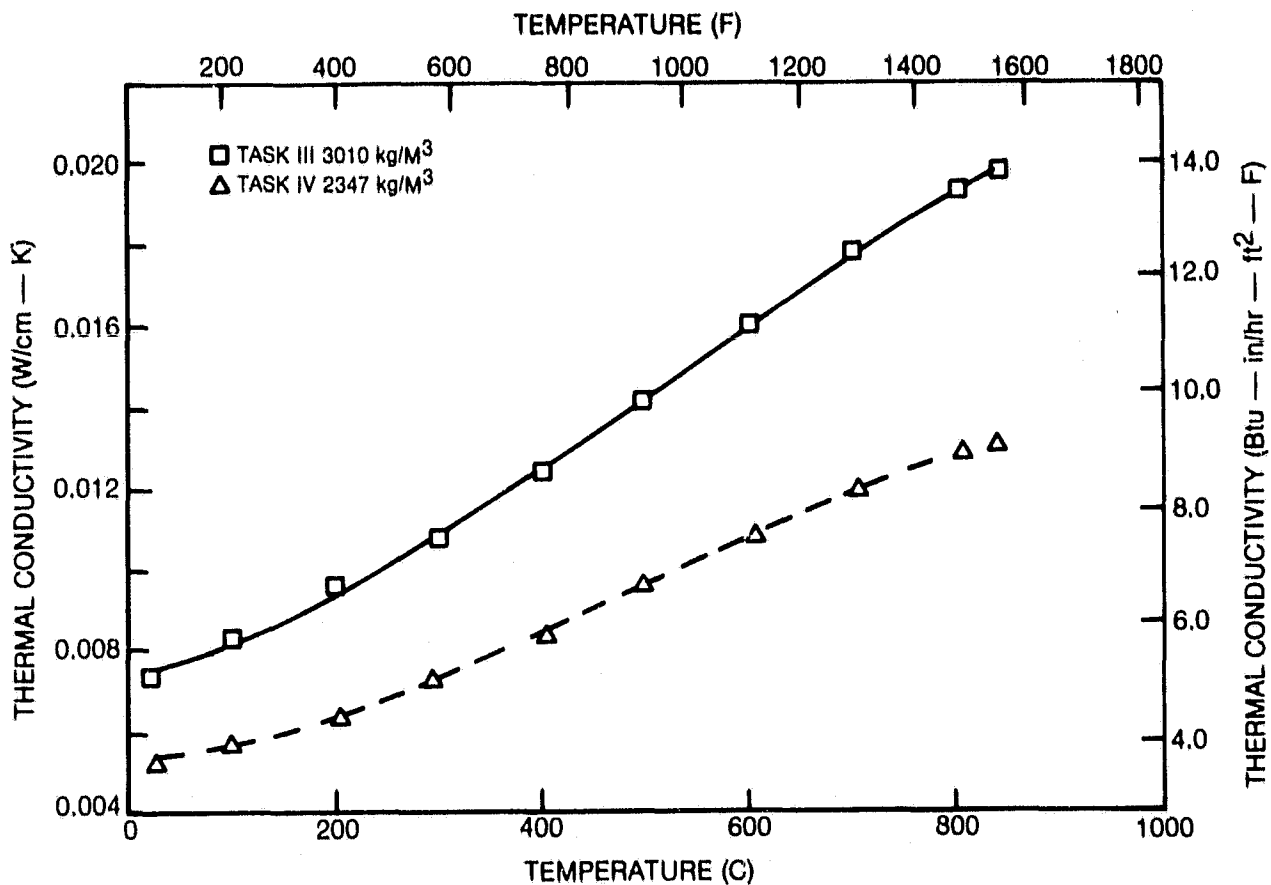
PLASMA SPRAYED NiCrAlY

DENSITY = 2347 Kg/M^3, AGED 500 hrs AT 1311°K

WHITE = METAL
LIGHT GREY = OXIDE
DARK GREY = MOUNTING MATERIAL

PARTIAL OXIDATION OF LARGE PARTICLES
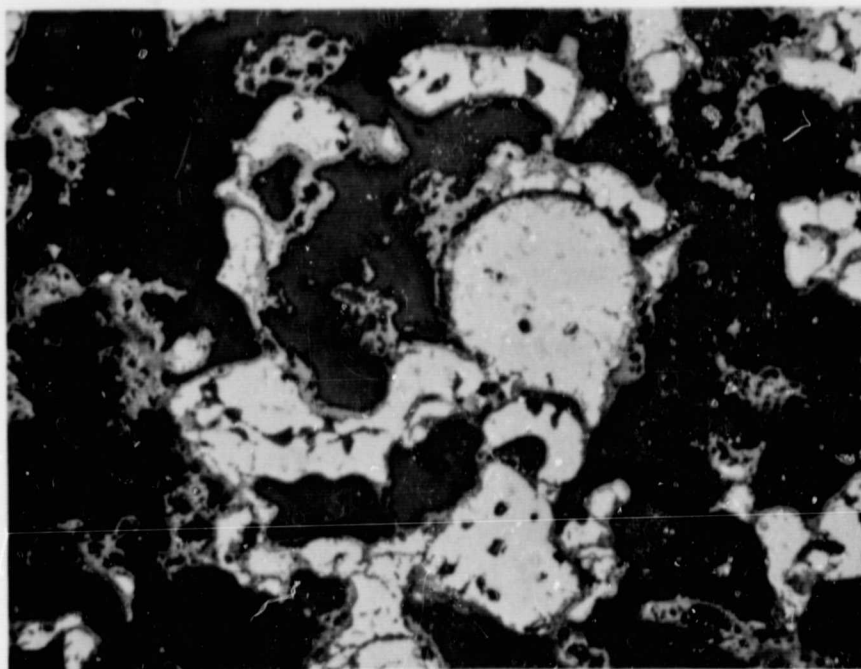
50μm

TOTAL OXIDATION OF SMALL PARTICLES

50μm

81-8-92-14

FIG. 5-7
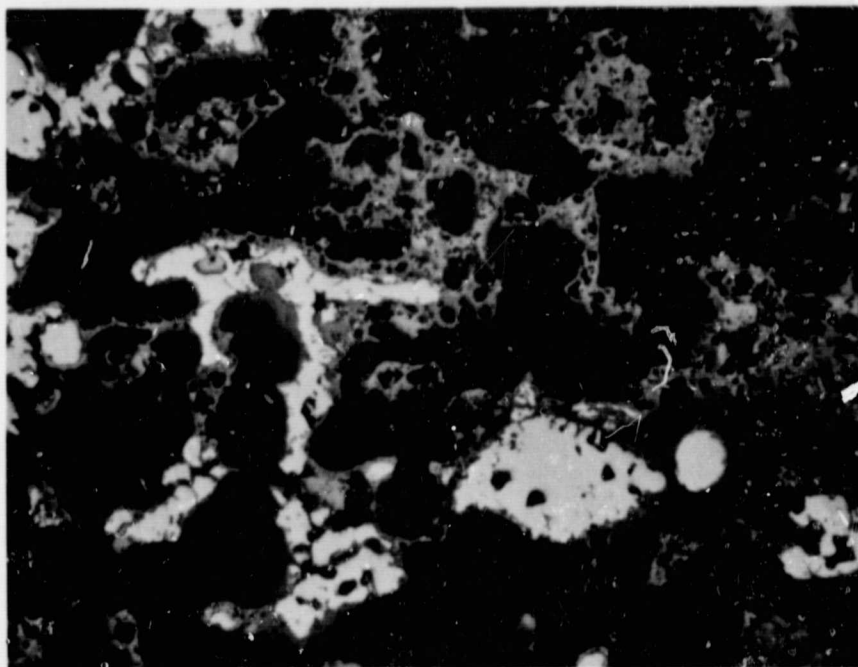
PLASMA SPRAYED NiCrAlY DENSITY 2347 Kg/M^3 AS-FABRICATED

UTRC81-043

LIGHT AREAS = METAL
DARK AREAS = POLYESTER

50μm

81-6-92-12
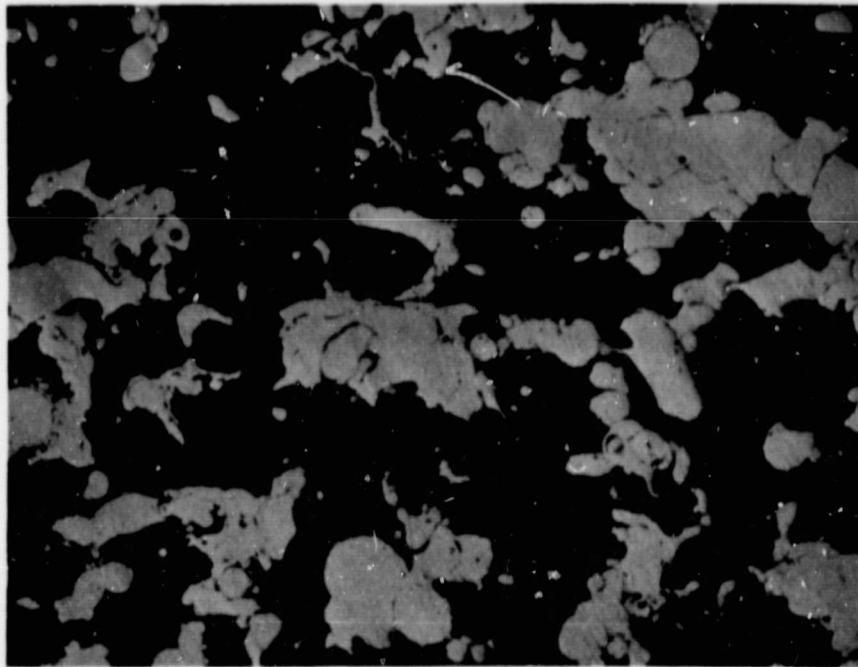
VI. CONCLUSIONS AND RECOMMENDATIONS FOR FUTURE WORK

6.1 Conclusions

1. All three canidate systems investigated in the program offer promise as low modulus interlayers, but each has features requiring further investigation.

2. Brunsbond[R] Pad has a good combination of room temperature properties and oxidation resistance, but the brazing operation for attachment is a disadvantage, and further testing of high temperature properties appears necessary.

3. The plasma sprayed porous NiCrAlY system exhibits oxidation and any swelling of the material must be evaluated for its effect on performance.

4. The microcracked zirconia system is interesting and offers attractive features, especially in regards to oxidation. However, the system must be thermally cycled in a strain isolator configuration in order to properly assess whether the microcrack structure is functional in accommodating strain.

6.2 Recommendations

1. Perform mechanical property tests on the systems of interest at the upper use temperature.

2. Measure the thermal expansion coefficients in the as-fabricated and aged conditions.

3. Examine the fatigue and creep properties of 35% dense Brunsbond[R] Pad at room and elevated temperatures.

4. Examine methods to decrease the effect of oxidation in the NiCrAlY system. This could include the application of a protective coating, fabrication under inert conditions, preoxidation prior to ceramic deposition, or examination of an alternate structure resistant to oxidation effects.

5. Perform limited thermal cycle testing on the zirconia system in a strain isolator configuration.

VII. REFERENCES

1. Shiembob, L. T.: "Development of Improved High Pressure Turbine Outer Gas Path Seal Components". NASA-CR-159801, January 1980.

2. Bill, R. C., D. W. Wisander, and D. E. Brewe: "Preliminary Study of Methods for Providing Thermal Shock Resistance to Plasma Sprayed Ceramic Gas Path Seals". NASA-TP-1561, May 1980.

3. Erickson, A. F., J. C. Nablo, and C. Pamzera: "Bonding Ceramic Material to Metallic Substrates for High-Temperature, Low-Weight Applications". ASME Paper 78-WA/GT-16, December 1978.

4. Mack, G.: "Turbine Ceramic Tip Seal". Air Force Contract No. F33615-79-C-2058.

5. "Metco 443 Nickel Chromium/Aluminum Composite Powders". Metco Technical Bulletin, January 1973, Metco Inc.,Westbury, N.Y.

6. Stecura, S.: "Effects of Yttrium, Aluminum and Chromium Concentrations in Bond Coatings on the Performance of Zirconia-Yttria Thermal Barriers". NASA-TM-79206, July 1979.

7. Tolokan, R. P., J. C. Nablo, and J. B. Brady: "Ceramic to Metal Attachment Using Low Modulus Brunsbond[R] Pad". ASME Paper 81-GT-160, December 1980.

8. Personal Communication with R. P. Tolokan, Brunswick Corporation, Technetics Division, Deland, Florida.

TABLE A-1

ROOM TEMPERATURE TENSILE TEST RESULTS ON BRUNSBOND^R PAD

TASK II

Brunswick Specimen Description	Density %	Strength MPa (KSI)	Modulus GPa (MSI)	Strain %
16647-1-2A-1	29.0	26.6 (3.86)	5.58 (.810)	≥2.0
16647-1-2A-2	29.6	25.5 (3.70)	7.86 (1.14)	3.2
16647-1-2A-3	31.4	18.9 (4.19)	9.24 (1.34)	≥ .82
Average	30.0	27.0 (3.92)	7.56 (1.09)	
16647-2-1A-1	34.99	34.7 (5.03)	8.96 (1.30)	≥1.0
16647-2-1A-2	36.2	43.1 (6.25)	12.8 (1.86)	≥1.38
16647-1-1A-3	35.06	37.0 (5.36)	13.4 (1.95)	≥1.64
Average	35.4	38.3 (5.55)	11.72 (1.70)	
16647-3-2B-1	39.2	45.4 (6.59)	18.2 (2.64)	≥1.06
16647-3-2B-2	37.7	45.3 (6.57)	16.3 (2.36)	3.69
16647-3-2B-3	42.9	35.9 (5.20)	10.7 (1.55)	≥1.63
Average	39.9	42.2 (6.12)	15.1 (2.18)	

TABLE A-2

MEASURED OXIDATION OF BRUNSBOND^R PAD

TASK II

(1311°K, 24 Hours, Static Air)

Specimen Description	Reference No.	Nominal Surface Area (m^2)	Wire Surface Area (m^2)	Pre-weight (kg)	Post-weight (kg)	----Oxidation----		
						Nominal Surface (kg/m^2)	Weight Percent (%)	Wire Surface (kg/m^2)
29.85% Fiber Metal	Brunswick 16647-1-2A#4	1.75×10^{-3}	1.40×10^{-2}	3.5247×10^{-3}	3.5408×10^{-3}	9.14×10^{-3}	+0.45	1.15×10^{-3}
35.85% Fiber Metal	Brunswick 16647-2-1A#4	1.71×10^{-3}	1.75×10^{-2}	4.4258×10^{-3}	$4.45-5 \times 10^{-3}$	1.46×10^{-3}	+0.56	1.41×10^{-3}
42.64% Fiber Metal	Brunswick 16647-3-2B#4	1.70×10^{-3}	2.00×10^{-2}	5.0704×10^{-2}	5.0989×10^{-3}	1.71×10^{-2}	+0.57	1.43×10^{-3}

PLASMA SPRAY PARAMETERS FOR POROUS NiCrAlY

Parameters	Setting		
Spray System	Metco 7M		
Powder Blend	Task II	(-170+325)NiCrAlY + 10% w/o Metco 600 ≡ 4750 kg/m^3	
(16 hr, °K bakeout)		(-170+325)NiCrAlY + 25% w/o Metco 600 ≡ 2870 kg/m^3	
		(-170+325)NiCrAlY + 30% w/o Metco 600 ≡ 2390 kg/m^3	
	Task III	(-100+200)NiCrAlY + 30% w/o Metco 600 ≡ 3010 kg/m^3	
	Task IV	(-100+200)NiCrAlY + 33% w/o Metco 600 ≡ 2347 kg/m^3	
Nozzle	7MG		
Gun Distance	75 mm		
Cooling Jets Cross Distance	150 mm		
Cooling Jets Pressure	20 psi		
Amperage	500		
Volts	70		
Horizontal Gun Speed	220 mm/sec		
Vertical increment	3 mm		
1° Arc Gas, Pressure, CFH	N_2, 50 psi, 100		
2° Arc Gas, Pressure, CFH	H_2, 50 psi, 5		
Powder Feed Rate	20 g/min		
Powder Port	2		
Deposition Rate	20 µm/cycle		
Total Deposition	3.75 mm		
Powder Used	2000 g/150 cm^2		

TABLE A-4

MECHANICAL PROPERTY DATA ON PLASMA SPRAYED POROUS NiCrAlY

TASK II

Reference No.	Bulk Density Kg/m³	4 pt. Strength MPa (KSI)		Modulus				4 pt. strain (%)
				Gage GPa (MSI)		Deflectometer GPa (MSI)		
UTRC 80-114	4780	87.0	(12.6)	52.2	(7.57)	23.4	(3.40)	0.20
UTRC 80-115	2870	19.5	(2.83)	10.5	(1.53)	6.21	(0.90)	0.21
UTRC 80-120	2390	13.2	(1.91)	5.29	(0.77)	--	--	0.35

TABLE A-5

OXIDATION DATA ON PLASMA SPRAYED POROUS NiCrAlY

TASK II

(1311°K for 24 Hours)

| Reference No. | Nominal Surface Area (m²) | Pre-weight* (Kg) | Post Weight (Kg) | ----------Oxidation---------- | |
				Nominal Surface (Kg/m²)	Percent Weight Change (%)
UTRC 80-114	1.57×10^{-3}	8.0228×10^{-3}	8.5083×10^{-3}	0.31	+ 6.1
UTRC 80-115	1.48×10^{-3}	$3.352^4 \times 10^{-3}$	3.6440×10^{-3}	0.20	+ 8.7
UTRC 80-120	1.56×10^{-3}	3.9746×10^{-3}	4.4013×10^{-3}	0.27	+10.7

*The pre-weight represents prior conditioning at 1000°F for 1 hour to remove wax, polyester and moisture.

TABLE A-6

LOW MODULUS CERAMIC 4-POINT BEND
PROPERTY TEST RESULTS AT ROOM TEMPERATURE

TASK II

Description	UTRC #	Strength		Gage		Deflectometer		Strain	Density
		MPa	(KSI)	GPa	(MSI)	GPa	(MSI)	ϵf (%)	ρ(Kg/m³)
Porous polyester	80-95	1.3	(.19)	3.8	(.55)	-	-	.05	2270
Microcracked	80-96	8.8	(1.3)	15.1	(2.2)	4.0	(.59)	.11	5090
Parameter Variation	80-98	12.7	(1.8)	14.7	(2.1)	4.5	(.66)	.11	4930

TABLE A-7

MEASURED OXIDATION OF LOW MODULUS CERAMIC

TASK II

(1311°K, 24 Hours, Static Air)

Specimen Description	Reference No.	Nominal Surface Area (m^2)	Original* Weight (kg)	Pre-weight* (kg)	Post-weight (kg)	Oxidation Nominal Surface (kg/m^2)	Oxidation Weight Percent (%)
Porous Polyester Zirconia	UTRC 80-95	1.68×10^{-3}	4.3293×10^{-3}	3.7090×10^{-3}	3.7030×10^{-3}	None	None
Microcracked zirconia	UTRC 80-96	1.68×10^{-3}	8.3462×10^{-3}	8.3327×10^{-3}	8.3315×10^{-3}	None	None
Parameter Variation Zirconia	UTRC 80-98	1.68×10^{-3}	7.9648×10^{-3}	7.9060×10^{-3}	7.9055×10^{-3}	None	None

*For the ceramic systems, the original weight represents the as-machined weight whereas the pre-weight represents prior conditioning at 1000°F for 1 hour to remove moisture and wax (and polyester in the case of specimen 80-95).

TABLE A-8

ROOM TEMPERATURE AND 1089°K MECHANICAL PROPERTY TEST DATA
ON 35% BRUNSBOND^R PAD IN THE AS-RECEIVED CONDITION

TASK III

Temperature (°K)	----Strength---- MPA	(KSI)	----Modulus---- GPA°	(MSI)°	Strain to Failure (%)
298	37.6	(5.46)	12.1	(1.76)	2.9
	33.0	(4.79)	9.72	(1.41)	2.0
	36.5	(5.30)	9.94	(1.44)	2.3
Avg.	35.7	(5.18)	10.58	(1.54)	2.4

Temperature (°K)	----Strength---- MPA	(KSI)	----Modulus---- GPA°	(MSI)°	Strain to P$_{max}$ (%)
1089°K	2.67	(.416)	4.33	(.628)	13.4
	4.32	(.626)	2.58	(.374)	13.4
	3.53	(.511)	3.96	(.574)	14.3
Avg.	3.57	(.518)	3.62	(.525)	13.7

o Extensometer

56

TABLE A-9

ROOM TEMPERATURE AND 1089°K MECHANICAL PROPERTY TEST DATA
ON 35% BRUNSBOND^R PAD AFTER THERMAL AGING AT 1311°K FOR 500 HOURS

TASK III

Temperature (°K)	----Strength----		----Modulus----		Strain to P_{max} (%)
	MPA	(KSI)	GPA°	(MSI)°	
298	49.0	(7.10)	5.82	(.845)	4.33
	39.4	(5.72)	6.15	(.893)	4.2
	36.4	(5.28)	13.9	(2.02)	.98
Avg.	41.6	(6.03)	8.62	(1.25)	3.17

Temperature (°K)	----Strength----		----Modulus----		Strain to P_{max} (%)
	MPA	(KSI)	GPA°	(MSI)°	
1089	5.11	(.741)	6.03	(.874)	3.11
	5.16	(.748)	16.4	(2.37)	10.66
	4.87	(.707)	6.53	(.947)	4.79
Avg.	5.05	(.732)	9.65	(1.40)	6.19

o Extensometer

TABLE A-10

ROOM TEMPERATURE AND 1089°K MECHANICAL PROPERTY TEST DATA ON POROUS NiCrAlY
(-100 + 200 MESH, UTRC 81-016) DENSITY = 3010 Kg/M³ IN THE AS-SPRAYED CONDITION

TASK III

Temperature (°K)	Strength MPA	(KSI)	Modulus Strain Gage GPA	(MSI)	Deflectometer GPA	(MSI)	Strain to to failure %
298	34.6	(5.02)	15.4	(2.24)	10.0	(1.46)	.35
	23.2	(3.36)	10.2	(1.49)	10.9	(1.58)	.34
	23.5	(3.41)	9.48	(1.38)	9.55	(1.39)	.36
	24.4	(3.54)	11.9	(1.73)	8.52	(1.24)	.31
Avg.	26.4	(3.83)	11.79	(1.71)	9.74	(1.41)	.34

Temperature (°K)	Strength MPA	(KSI)	Modulus Deflectometer GPA	(MSI)
1089	17.6	(2.55)	6.80	(.986)
	20.1	(2.91)	5.95	(.863)
	18.0	(2.62)	7.48	(1.08)
Avg.	18.6	(2.69)	6.74	(.976)

TABLE A-11

ROOM TEMPERATURE AND 1089°K MECHANICAL PROPERTY DATA ON POROUS
NiCrAlY (-100 + 200 MESH, UTRC 81-016) DENSITY = 3010 Kg/M^3
AFTER AGING AT 1311°K FOR 500 HOURS

TASK III

Temperature (°K)	Strength		Modulus — Strain Gage		Modulus — Deflectometer		Strain to Failure %
	MPA	(KSI)	GPA	(MSI)	GPA	(MSI)	
298	38.8	(5.63)	30.2	(4.37)	25.0	(3.62)	.159
	47.6	(6.90)	30.6	(4.44)	20.9	(3.03)	.184
	58.6	(8.50)	37.7	(5.47)	24.0	(3.38)	.207
Avg.	48.3	(7.01)	32.8	(4.76)	23.3	(3.38)	.183

Temperature (°K)	Strength		Modulus — Deflectometer	
	MPA	(KSI)	GPA	(MSI)
1089	37.2	(5.40)	19.7	(2.85)
	46.1	(6.69)	16.9	(2.45)
	35.8	(5.20)	20.4	(2.96)
Avg.	39.8	(5.76)	19.0	(2.75)

TABLE A-12

ROOM TEMPERATURE AND 1089°K MECHANICAL PROPERTIES OF AS-SPRAYED MICROCRACKED ZIRCONIA (80-129)

TASK III

| Temperature (°K) | —Strength— | | —————Modulus————— | | | | Strain Failure % |
	MPA	(KSI)	GPA*	(MSI)*	GPA+	(MSI)+	
298	11.1	(1.61)	31.4	(4.56)	8.35	(1.21)	.088
	8.91	(1.29)	6.18	(.896)	4.85	(.70)	.128
	9.08	(1.32)	15.4	(2.23)	4.68	(.68)	.129
Avg.	9.69	(1.41)	17.7	(2.56)	5.96	(.86)	.115
1089	11.3	(1.64)			2.97	(.431)	
	12.3	(1.79)			3.73	(.541)	
	12.5	(1.82)			3.62	(.524)	
Avg.	12.0	(1.73)			3.44	(.499)	

* Strain Gage

+ Deflectometer

TABLE A-13

ROOM TEMPERATURE AND 1089°K MECHANICAL PROPERTY TEST DATA
ON MICROCRACKED ZIRCONIA (80-129) AFTER THERMAL AGING AT 1311°K FOR 500 HOURS

TASK III

Temperature (°K)	Strength		Modulus				Strain to Failure (%)
	MPA	(KSI)	GPA*	(MSI)*	GPA+	(MSI)+	
298	10.7	(1.55)	38.5	(5.59)	19.1	(2.77)	.07
	12.3	(1.78)	26.8	(3.88)	15.8	(2.30)	.09
	10.4	(1.52)	29.3	(4.24)	16.1	(2.33)	.07
Avg.	11.13	(1.61)	31.5	(4.57)	17.0	(2.46)	.08
1089	10.5	(1.53)			8.52	(1.24)	
	16.4	(2.83)			12.8	(1.85)	
	12.6	(1.82)			9.72	(1.41)	
Avg.	13.2	(2.06)			10.3	(1.50)	

* Strain Gage
+ Deflectometer

TABLE A-14

WEIGHT AND DIMENSION CHANGES OF 35% DENSE BRUNSBOND^R PAD VERSUS TIME AT 1311°K

TASK III

	Dimensional Change (%)		Weight Change %
Time (Hrs.)	X-Y plane*	Z-Axis**	
1	+.60	+1.9	+ .34
10	+.20	0	+ .40
100	+.53	+1.9	+ .81
200	-.20	+3.8	+ .80
500	+.20	-1.0	+1.30

* ± 1 mil change = ± .2%

** Z - Axis is thickness direction (100 mils), ± 1 mil change = ± 1%.

TABLE A-15

WEIGHT AND DIMENSION CHANGES OF 35%
BRUNSPOND[R] PAD VEPSUS TIME AS THE RESULT OF THERMAL
CYCLE TESTING BETWEEN RT AND 1311°K

TASK III

Time @ 1311°K(Hr)	---Dimensional Change (%) ---		Weight Change (%)
	X-Y Plane	Z Plane	
1	< .1	< 1	+ .18
10	< .1	< 1	+ .36
50	< .1	< 1	+ .54
100	.2	1	+ .65

TABLE A-16

WEIGHT AND DIMENSION CHANGES OF POROUS NiCrAlY (-100 + 200 MESH, UTRC 81-016) DENSITY = 3010 Kg/M^3 VERSUS TIME AT 1311°K

TASK III

Dimensional Change (%)*

Time (Hrs.)	X-Y plane**	Z - Axis***	Weight Change %
1	0	-2.6	+ 1.8
10	0	0	+ 3.1
100	+.06	0	+ 6.9
200	+.33	-1.0	+ 8.2
500	+1.4	+1.8	+10.5

* X-Y plane is perpendicular to Spray Axis, Z - Axis is parallel

** ± 1 mil change = ± .2%

*** ± 1 mil change ± 1%

TABLE A-17

WEIGHT AND DIMENSIONAL CHANGE MEASUREMENTS OF POROUS NiCrAlY
(-100 + 200 MESH, UTRC 81.-016) DENSITY = 3010 Kg/M^3
VERSUS TIME AS THE RESULT OF THERMAL CYCLE TESTING
BETWEEN RT AND 1311°K

TASK III

Time @ 1311°K (hr)	---Dimensional Change--- (%)*		Weight Change %
	X-Y plane**	Z - Axis***	
1	0	0	+2.8
10	+.59	+1.9	+6.0
50	+.66	+1.9	+7.3
100	+.99	+1.9	+8.3

*X-Y plane = plane perpendicular to spray axis, Z
axis = direction parallel to spray axis

**± 1 mil change = ± .2%
*** ± 1 mil change in thickness = ± 1%

TABLE A-18

WEIGHT AND DIMENSION CHANGES OF MICROCRACKED
ZIRCONIA (80-129) VERSUS TIME AT 1311°K

TASK III

Time (Hrs)	% Change Length (in.)	% Change Width (in.)	% Change Depth (in.)	% Change Weight (g)
0	(1.00)	(.998)	(.100)	(8.47714)
1	0	0	0	0
10	0	0	0	0
106	0	0	0	0
268	0	0	0	0
500	0	0	0	0

TABLE A-19

WEIGHT AND DIMENSIONAL CHANGE MEASUREMENTS OF MICROCRACKED
ZIRCONIA (80-129) VERSUS TIME AS THE RESULT OF THERMAL
CYCLE TESTING BETWEEN RT AND 1311°K

TASK III

| Time @ 1311°K (Hr) | ---Dimensional Change (%)* --- | | Weight Change % |
	X-Y Plane	Z Plane	
1	< .1	< 1	+ .005
10	< .1	< 1	− .005
50	< .1	< 1	− .003
100	.3	< 1	−0.0076

*X-Y Plane = plane perpendicular to spray axis
 Z Plane = plane parallel to spray axis

TABLE A-20

SPECIFIC HEAT OF TASK III CANDIDATES
(From TPRL 249, Taylor & Groot)

Temp. (°K)	Temp. (°C)	Temp. (°F)	Zirconia (Ws gm^{-1}K^{-1})	NiCrAlY (Ws gm^{-1}K^{-1})	Fiber Metal (Ws gm^{-1}K^{-1})
340	67	152	0.4836	0.4761	0.5011
350	77	170	0.4890	0.4769	0.5081
375	102	215	0.5031	0.4818	0.5206
400	127	260	0.5143	0.4843	0.5314
425	152	305	0.5252	0.4880	0.5426
450	177	350	0.5363	0.4914	0.5537
475	202	395	0.5445	0.4959	0.5650
500	227	440	0.5527	0.5000	0.5740
525	252	485	0.5607	0.5062	0.5891
550	277	530	0.5668	0.5107	0.6005
575	302	575	0.5724	0.5169	0.6128
600	327	620	0.5768	0.5230	0.6245
625	352	665	0.5818	0.5299	0.6357
650	377	710	0.5849	0.5384	0.6454
675	402	755	0.5917	0.5459	0.6584
700	427	800	0.5969	0.5531	0.6624
725	452	845	0.6026	0.5612	0.6909
750	477	890	0.6083	0.5731	0.7244
775	502	935	0.6137	0.5831	0.7661
800	527	980	0.6153	0.5925	0.8243
825	552	1025	0.6200	0.6030	0.8172
850	577	1070	0.6251	0.6141	0.7812
875	602	1115	0.6275	0.6261	0.7472
900	627	1160	0.6285	0.6331	0.7306
925	652	1205	0.6317	0.6421	0.7162
950	677	1250	0.6345	0.6521	0.6988
975	702	1295	0.6357	0.6632	0.6806

TABLE A-21

THERMAL DIFFUSIVITY OF TASK III CANDIDATES
(From TPRL 249, Taylor & Groot)

Sample Name	Temp. (°C)	Diffusivity $(cm^2 \, sec^{-1})$
Zirconia	23	0.00435
	80	0.00390
	199	0.00352
	322	0.00339
	463	0.00326
	611	0.00320
	730	0.00313
	842	0.00294
NiCrAlY	23	0.00594
	85	0.00533
	200	0.00610
	334	0.00728
	465	0.00782
	598	0.00851
	742	0.00951
	751	0.00906
	848	0.00917
Fiber Metal	23	0.00780
	127	0.00789
	254	0.00807
	376	0.00884
	497	0.00876
	626	0.01030
	722	0.01132
	815	0.01302

TABLE A-22

THERMAL CONDUCTIVITY OF TASK III CANDIDATES
(From TPRL 249, Taylor & Groot)

Sample Name	Temp. (°C)	Density (gm cm⁻³)	Specific Heat (Ws gm⁻¹ K⁻¹)	Diffusivity (cm² sec⁻¹)	Conductivity (W cm⁻¹ K⁻¹)	Conductivity (BTU in hr⁻¹ ft⁻² F⁻¹)	Temp. (°F)
Zirconia	23	5.2180	0.462	0.00435	0.01049	7.27	73
	100	5.2180	0.503	0.00382	0.01003	6.95	212
	200	5.2180	0.544	0.00352	0.00999	6.93	392
	300	5.2180	0.572	0.00339	0.01012	7.02	572
	400	5.2180	0.592	0.00330	0.01019	7.07	752
	500	5.2180	0.614	0.00323	0.01035	7.17	932
	600	5.2180	0.624	0.00316	0.01029	7.13	1112
	700	5.2180	0.636	0.00311	0.01032	7.16	1292
	800	5.2180	0.645	0.00304	0.01023	7.09	1472
	843	5.2180	0.647	0.00301	0.01016	7.05	1550
NiCrAlY	23	3.0263	0.464	0.00525	0.00737	5.11	73
	100	3.0263	0.482	0.00570	0.00831	5.76	212
	200	3.0263	0.496	0.00636	0.00955	6.62	392
	300	3.0263	0.517	0.00689	0.01078	7.47	572
	400	3.0263	0.546	0.00750	0.01239	8.59	752
	500	3.0263	0.583	0.00801	0.01413	9.80	932
	600	3.0263	0.626	0.00846	0.01603	11.11	1112
	700	3.0263	0.663	0.00891	0.01788	12.40	1292
	800	3.0263	0.689	0.00930	0.01939	13.45	1472
	843	3.0263	0.697	0.00944	0.01991	13.81	1550
Fiber Metal	23	2.684	0.475	0.00780	0.00994	6.89	73
	100	2.684	0.521	0.00785	0.01098	7.61	212
	200	2.684	0.565	0.00800	0.01213	8.41	392
	300	2.684	0.613	0.00826	0.01359	9.42	572
	400	2.684	0.658	0.00858	0.01515	10.51	752
	500	2.684	0.766	0.00900	0.01850	12.83	932
	600	2.684	0.747	0.01006	0.02017	13.98	1112
	700	2.684	0.681	0.01113	0.02034	14.11	1292
	800	2.684	0.710	0.01267	0.02414	16.74	1472
	843	2.684	0.720	0.01345	0.02599	18.02	1550

TABLE A-23

AS SPRAYED, ROOM TEMPERATURE AND 1089°K MECHANICAL
PROPERTY MEASUREMENTS ON POROUS NiCrAlY
(UTRC 81-043) DENSITY 2347 Kg/M^3

TASK IV

Temp.	Strength		Modulus				Strain to Pmax %
	MPa	(KSI)	GPa$^+$ (MSI)$^+$		GPa*(MSI)*		
298°K	11.7	(1.69)	3.80	(.55)	7.02	(1.02)	.163
	10.5	(1.52)	2.91	(.42)	4.08	(.59)	.527
	11.5	(1.66)	2.17	(.31)	5.95	(.86)	.191
Ave.	11.2	(1.62)	2.96	(.43)	5.68	(.825)	.294
1089°K	9.14	(1.33)	2.71	(.393)	-	-	-
	7.89	(1.14)	1.43	(.208)	=	=	-
	7.11	(1.03)	1.17	(.170)	-	-	-
Ave.	8.05	(1.17)	1.77	(.257)			

+Deflectometer
* Strain Gage

TABLE A-24

ROOM TEMPERATURE AND 1089°K MECHANICAL PROPERTY MEASUREMENTS
ON POROUS NiCrAlY (UTRC 81-043) DENSITY 2347 Kg/M^3
AFTER AGING 500 HRS. AT 1311°K

TASK IV

Temp.	Strength		Modulus		Strain to Pmax
	MPa	(KSI)	GPa[+](MSI)[+]	GPa[*] (MSI)[*]	%
298°K	25.6	(3.72)	10.5 (1.53)	19.3 (2.80)	.179
	17.7	(2.57)	8.9 (1.29)	13.5 (1.96)	.162
	18.0	(2.61)	15.9 (2.30)	20.1 (2.91)	.106
Ave.	20.4	(2.97)	11.8 (1.71)	17.6 (2.56)	.149
1089°K	13.0	(1.89)	10.0 (1.45)		
	11.4	(1.66)	13.0 (1.88)		
Ave	12.2	(1.78)	11.5 (1.67)		

+Deflectometer

*Strain gage

TABLE A-25

STATIC OXIDATION OF POROUS NiCrAlY
(DENSITY = 2347 Kg/M^3) at 1311°K, WEIGHT AND
DIMENSION CHANGES VERSUS TIME

TASK IV

Time at 1311°K (hrs.)	Weight Change %	Dimension Change %		
		Height	Length	Width
1	+ 1.70	0	+ .19	0
10	+ 3.87	0	+ .39	+ .53
100	+ 9.33	0	- .19	+1.55
200	+11.01	0	+1.17	+1.55
500	+16.2	+4.39	+2.58	+2.51

TABLE A-26

CYCLIC OXIDATION OF POROUS NiCrAlY
(DENSITY = 2347 kg/M^3) BETWEEN ROOM TEMPERATURE
AND 1311°K

TASK IV

Time at 1311°K (hrs.)	Weight Change %	Dimension Change %		
		Height*	Length**	Width**
1	+ 2.47	- .95	- .59	- .53
10	+ 3.03	0	.19	0
50	+ 7.58	-1.88	+ .39	+ .52
100	+ 7.99	+1.75	+2.50	+1.28

*   ± 1 mil = ±1%

**   ± 1 mil = ~±.3%

TABLE A-27

SPECIFIC HEAT OF NiCrAlY
(From TPRL249A, Taylor & Groot)

Temp. (°K)	Temp. (°C)	Temp. (°F)	3010 Kg/M³ Task III NiCrAlY (Ws gm⁻¹K⁻¹)	2347 Kg/M³ Task IV NiCrAlY (Ws gm⁻¹K⁻¹)
315	42	108	--	0.4737
320	47	117	--	0.4753
325	52	126	--	0.4766
340	67	152	0.4761	--
350	77	170	0.4769	0.4757
375	102	215	0.4818	0.4864
400	127	260	0.4843	0.4908
425	152	305	0.4880	0.4900
450	177	350	0.4914	0.4928
475	202	395	0.4959	0.4932
500	227	440	0.5000	0.4948
525	252	485	0.5062	0.4973
550	277	530	0.5107	0.5003
575	302	575	0.5169	0.5080
600	327	620	0.5230	0.5193
625	352	665	0.5299	0.5246
650	377	710	0.5384	0.5360
675	402	755	0.5459	0.5416
700	427	800	0.5531	0.5512
725	452	845	0.5612	0.5598
750	477	890	0.5731	0.5711
775	502	935	0.5831	0.5812
800	527	980	0.5925	0.5903
825	552	1025	0.6030	0.5984
850	577	1070	0.6141	0.6110
875	602	1115	0.6261	0.6212
900	627	1160	0.6331	0.6313
925	652	1205	0.6421	0.6414
950	677	1250	0.6521	0.6498
975	702	1295	0.6632	0.6610

TABLE A-28

THERMAL DIFFUSIVITY OF NiCrAlY
(From TPRL249A, Taylor & Groot)

Sample	Temp. (°C)	Diffusivity (cm^2 sec^{-1})
NiCrAlY	23	0.00594
3010 Kg/M^3	85	0.00533
Task III	200	0.00610
	334	0.00728
	465	0.00782
	598	0.00851
	742	0.00951
	751	0.00906
	848	0.00917
NiCrAlY	22	0.00435
2347 Kg/M^3	300	0.00541
Task IV	664	0.00690
	838	0.00740

TABLE A-29

THERMAL CONDUCTIVITY OF NiCrAlY

(From TPRL249A, Taylor & Groot)

Sample Name	Temp. (°C)	Density (gm cm⁻³)	Specific Heat (Ws gm⁻¹K⁻¹)	Diffusivity (cm² sec⁻¹)	Conductivity (W cm⁻¹ K⁻¹)	Conductivity (Btu in hr⁻¹ft⁻²F⁻¹)	Temp. (°F)
NiCrAlY 3010 Kg/M³ Task III	23	3.0263	0.464*	0.00525*	0.00737	5.11	73
	100	3.0263	0.482	0.00570	0.00831	5.76	212
	200	3.0263	0.496	0.00636	0.00955	6.62	392
	300	3.0263	0.517	0.00689	0.01078	7.47	572
	400	3.0263	0.546	0.00750	0.01239	8.59	752
	500	3.0263	0.583	0.00801	0.01413	9.80	932
	600	3.0263	0.626	0.00846	0.01603	11.11	1112
	700	3.0263	0.663	0.00891	0.01788	12.40	1292
	800	3.0263	0.689	0.00930	0.01939	13.45	1472
	843	3.0263	0.697	0.00944	0.01991	13.81	1550
NiCrAlY 2347 Kg/M³ Task IV	23	2.5303	0.464*	0.00425*	0.00498	3.46	73
	100	2.5303	0.482	0.00463	0.00564	3.91	212
	200	2.5303	0.496	0.00506	0.00634	4.41	392
	300	2.5303	0.517	0.00548	0.00716	4.97	572
	400	2.5303	0.546	0.00592	0.00817	5.67	752
	500	2.5303	0.583	0.00635	0.00936	6.50	932
	600	2.5303	0.626	0.00683	0.01081	7.50	1112
	700	2.5303	0.663	0.00715	0.01199	8.3]	1292
	800	2.5303	0.689	0.00735	0.01281	8.89	1472
	843	2.5303	0.697	0.00740	0.01305	9.05	1550

* smoothed values